

1 **Palaeoecology, taphonomy, and preservation of a lower Pliocene shell bed**
2 **(coquina) from a volcanic oceanic island (Santa Maria Island, Azores)**

3

4 Sérgio P. Ávila ^{1,2,3,4}, Ricardo S. Ramalho ^{5,6}, Jörg M. Habermann ⁷, Rui Quartau ^{8,9},
5 Andreas Kroh ¹⁰, Björn Berning ¹¹, Markes Johnson ¹², Michael X. Kirby ¹³, Vittorio
6 Zanon ¹⁴, Jürgen Titschack ¹⁵, Adam Goss ¹⁶, Ana Cristina Rebelo ^{2,3,4}, Carlos Melo ^{3,19},
7 Patrícia Madeira ^{2,3,4}, Ricardo Cordeiro ^{2,3,4}, Ricardo Meireles ^{2,3,4}, Leila Bagaço ^{3,4}, Ana
8 Hipólito ¹⁴, Alfred Uchman ¹⁷, Carlos Marques da Silva ^{9,18}, Mário Cachão ^{9,18}, José
9 Madeira ^{9,18}

10

11

12 ¹ *Faculdade de Ciências da Universidade do Porto, Rua do Campo Alegre, Porto,*
13 *Portugal*

14 ² *CIBIO, Centro de Investigação em Biodiversidade e Recursos Genéticos, InBIO*
15 *Laboratório Associado, Pólo dos Açores, Açores, Portugal*

16 ³ *Departamento de Biologia, Universidade dos Açores, 9501-801 Ponta Delgada,*
17 *Açores, Portugal*

18 ⁴ *MPB-Marine PalaeoBiogeography Working Group of the University of the Azores,*
19 *Rua da Mãe de Deus, 9501-801*

20 ⁵ *School of Earth Sciences, University of Bristol, Wills Memorial Building, Queen's*
21 *Road, Bristol, BS8 1RJ, UK*

22 ⁶ *Lamont-Doherty Earth Observatory at Columbia University, Comer Geochemistry*
23 *Building, 61 Route 9W/ PO box 1000, Palisades, NY-10964-8000, USA.*

24 ⁷ *GeoZentrum Nordbayern, Universität Erlangen-Nürnberg, Schloßgarten 5, 91054*
25 *Erlangen, Germany*

26 ⁸ *Divisão de Geologia Marinha e Georecursos, Instituto Português do Mar e da*
27 *Atmosfera I.P., Rua C do Aeroporto, 1749-077 Lisboa, Portugal*

28 ⁹ *Instituto Dom Luiz, Faculdade de Ciências da Universidade de Lisboa, Campo*
29 *Grande, Edifício C8, Piso 3, 1749-016 Lisboa, Portugal*

30 ¹⁰ *Naturhistorisches Museum Wien, Geologisch-Paläontologische Abteilung, Burggring*
31 *7, 1010 Wien, Austria*

32 ¹¹ *Oberösterreichisches Landesmuseum, Geowissenschaftliche Sammlungen, Welser Str.*
33 *20, 4060 Leonding, Austria*

34 ¹² *Department of Geosciences, Williams College, Williamstown, Massachusetts 01267*
35 *USA*

36 ¹³ *Anacapa Paleo Resources, 363 Woodley Road, Santa Barbara, CA 93108, USA*

37 ¹⁴ *Centro de Vulcanologia e Avaliação de Riscos Geológicos, Universidade dos Açores,*
38 *9501-801 Ponta Delgada, Açores, Portugal*

39 ¹⁵ *Senckenberg am Meer, Abteilung Meeresforschung, Südstrand 40, 26382*
40 *Wilhelmshaven, Germany*

41 ¹⁶ *ExxonMobil Upstream Research, 3120 Buffalo Speedway, Houston, TX, 77098, USA*

42 ¹⁷ *Institute of Geological Sciences, Jagiellonian University, Oleandry 2a; PL 30-063*
43 *Kraków, Poland*

44 ¹⁸ *Departamento de Geologia, Faculdade de Ciências da Universidade de Lisboa, 1749-*
45 *016 Lisboa, Portugal*

46 ¹⁹ *Departamento de Geociências, Universidade dos Açores, 9501-801 Ponta Delgada,*
47 *Açores, Portugal*

48

49 *** Corresponding author, e-mail address: avila@uac.pt (Sérgio Ávila).**

50

51 **ABSTRACT**

52 Massive fossil shell accumulations require particular conditions to be formed and may
53 provide valuable insights into the sedimentary environments favouring such
54 concentrations. Shallow-water shell beds appear to be particularly rare on reefless
55 volcanic oceanic islands on account of narrow, steep and highly-energetic insular
56 shelves where the potential for preservation is limited. The occurrence of an exceptional
57 coquina (Pedra-que-pica) within the Miocene–Pliocene deposits of Santa Maria Island
58 (Azores), therefore provides a rare opportunity to understand the conditions that led to
59 the formation and preservation of a massive shell bed at mid-ocean insular setting. This
60 study provides a detailed analysis regarding a 10–11 m-thick bivalve-dominated fossil
61 assemblage exposed at Pedra-que-pica on Santa Maria Island in the Azores. Integration
62 of taphonomical, palaeoecological and sedimentological observations are used to
63 reconstruct the genesis of the coquina bed and related events, and to discuss why such
64 exceptional sedimentary bodies are so rare on shelves around reefless volcanic oceanic
65 islands.

66 The sequence at Pedra-que-pica demonstrates a complex succession of sedimentary
67 environments in response to the drowning of an existing coastline during a period of
68 rapid sea-level rise. The Pedra-que-pica shell bed incorporates storm-related materials
69 and possible debris falls that originated nearby in a shallow and highly productive
70 carbonate factory. Deposition took place below fair-weather wave base, at around 50 m
71 depth, as inferred from the overlying volcanic succession. The preservation of this
72 coquina was favoured by deposition on a platform laterally protected by a rocky spur,
73 combined with rapid burial by water-settled volcanic tuffs and subsequent volcanic
74 effusive sequences. The recent exhumation of the deposit is the result of island uplift
75 and subsequent erosion.

76

77

78 *Keywords:* Coquina, Sedimentary processes, Palaeoenvironmental reconstruction, Island

79 shelves, Volcanic oceanic islands, Azores.

80

81 **1. Introduction**

82 Coastlines at volcanic oceanic islands are extremely dynamic geomorphological
83 features, as they are subjected to vertical displacements over time (both subsidence and
84 uplift), to glacio-eustatic sea-level changes, are impacted by high-energy oceanic
85 conditions, and are frequently disturbed by medium- to large-scale geological processes
86 (i.e. landslides, active tectonics, volcanic eruptions, tsunamis, etc.) (Moore et al., 1989;
87 Schmincke, 2004; Felton et al., 2006; Crook and Felton, 2008; Quartau et al., 2010,
88 2012; Quartau and Mitchell, 2013; Ramalho et al., 2013). Around young and exposed
89 volcanic islands, sediment accommodation space is limited by narrow and shallow
90 shelves. The residence time of sediments on the shelves is very brief due to frequent
91 offshore transport induced by storms and sediment spill-over to the submarine slopes,
92 both reinforced during sea level drops (Tsutsui et al., 1987; Donovan, 2002; Ávila et al.,
93 2008a; Quartau et al., 2010, 2012, 2015; Ávila, 2013; Meireles et al., 2013). Due to the
94 subsidence trend to which most volcanic oceanic islands are subjected and at latitudes
95 where protective coral reef barriers fail to develop, the aforementioned conditions are
96 responsible for the scarcity and relative improbability for the retention of subaerial
97 exposures of thick, well-developed marine shelf deposits within island successions.
98 Only the most erosion-resistant deposits – hydrodynamically-stable coarse sediment
99 deposits such as boulder accumulations or well-lithified deposits – may withstand
100 shoreline transgressive-regressive cycles of sea-level changes (Felton et al., 2006; Ávila
101 et al., 2008a; Quartau et al., 2012). However, looser and finer shelf sediments have the
102 potential to be incorporated into an island edifice by volcanic progradation. The rare
103 islands that experienced uplift trends may thus exhibit well-preserved volcanic and
104 sedimentary marine sequences, thus constituting prime localities to gain insight
105 regarding sedimentation on volcanic island shelves.

106 The small island of Santa Maria (97 km²) in the Azores archipelago (North Atlantic
107 Ocean) is one of those exceptional cases. The fortuitous combination of uplift, coastal
108 erosion and volcanism (Serralheiro et al., 1987; Serralheiro and Madeira, 1990;
109 Serralheiro, 2003) resulted in the preservation and exposure of rich Neogene
110 fossiliferous marine sediments (Ferreira, 1955; Zbyszewski and Ferreira, 1962; Ávila et
111 al., 2002, 2009a, 2009b, 2010, 2012; Estevens and Ávila, 2007; Janssen et al., 2008;
112 Kroh et al., 2008; Winkelmann et al., 2010; Madeira et al., 2007, 2011; Meireles et al.,
113 2012), together with marine volcanic sequences (Serralheiro, 2003; Meireles et al.,
114 2013; Ramalho et al., 2013).

115 The focus of this study is the Pedra-que-pica (literally, “stone that stings”)
116 fossiliferous outcrop, which is located on the southeastern coast of Santa Maria Island.
117 Although previous work based on strontium-isotope stratigraphy suggested an
118 uppermost Miocene age for the deposit with an average estimated age of 5.51 ± 0.21 Ma
119 (Kirby et al., 2007), recent K/Ar datings indicate an age ranging between 4.02 ± 0.06 Ma
120 and 3.96 ± 0.06 Ma, thus early Pliocene in age (Sibrant et al., 2015). The sedimentary
121 sequence at Pedra-que-pica comprises a thick coquina unit – a sedimentary rock
122 composed of transported, abraded and mechanically sorted fragments of various origins
123 and entire shells of molluscs and other bioclasts that constitute > 50% of the rock
124 volume (Neuendorf et al., 2005). While such deposits are typically more abundant along
125 continental shores [e.g., east coast of Florida and southeastern North Carolina, both in
126 the USA (Fallaw, 1973); the Guadalquivir Basin, in Cadiz and the southern part of
127 Sevilla province, Spain (Aguirre, 1995)], they are rare in volcanic oceanic islands. In
128 fact, in the Atlantic Ocean, well-developed coquinas are only known from Santiago
129 Island (Cape Verde Archipelago – Serralheiro, 1976) and Santa Maria Island (Azores –
130 Serralheiro et al., 1987; Serralheiro and Madeira, 1990; Serralheiro, 2003; Kirby et al.,

131 2007). To our knowledge, the outcrop at Pedra-que-pica is possibly one of the world's
132 largest coquina shelf deposits in a volcanic oceanic island setting. Therefore, Santa
133 Maria represents an excellent opportunity to gain insights into the sedimentary
134 dynamics leading to coquina-bed formation on the exposed shelves of volcanic oceanic
135 islands and their preservation. To achieve this goal, a comprehensive analysis of the
136 outcrop from an integrated volcanostratigraphic, geomorphological, sedimentological,
137 petrographical, ichnological and palaeontological point of view was performed in order
138 to improve previous interpretations of the coquina (e.g., Kirby et al., 2007) and the
139 physical setting in which it accrued. The main aims of the present study are to
140 reconstruct and interpret the palaeoenvironment of the sedimentary sequence and
141 advance the understanding of the interplay of sedimentological, volcanological and
142 biological processes in producing and preserving such unusual sedimentary bodies on
143 reefless volcanic oceanic island shelves.

144

145

146 **2. Geological setting**

147 Located in the NE Atlantic Ocean, the Azores archipelago comprises nine volcanic
148 oceanic islands younger than 6 Ma (Ramalho et al., 2014; Sibrant et al., 2015). The
149 islands represent the emerged tops of larger volcanic edifices superimposed on the
150 Azores Plateau (Needham and Franchetau, 1974; Madeira and Ribeiro, 1990; Beier et
151 al., 2012; Fig. 1), a large area of elevated seafloor adjacent to the triple junction
152 between the Eurasian, Nubian and North American plates (Laughton and Whitmarsh,
153 1974; Schilling, 1975; Cannat et al., 1999; Gente et al., 2003; Marques et al., 2013).
154 With the exception of the south-eastern-most and oldest island (Santa Maria), none of

155 the other islands record exposed marine fossiliferous sequences (Serralheiro, 2003;
156 Quartau et al., 2014).

157 Santa Maria was the first island of the Azores to have emerged above sea level
158 during the late Miocene (Abdel-Monem et al., 1975). Its detailed volcanostratigraphic
159 sequence was defined by Serralheiro et al. (1987) and subsequently refined by
160 Serralheiro and Madeira (1990), Serralheiro (2003) and Ávila et al. (2012). The
161 geological evolution of Santa Maria can be summarised as follows (cf. Fig. 2): 1)
162 emergence of the volcanic edifice above sea-level during the Late Miocene
163 (Cabrestantes and Porto formations); 2) construction of a subaerial shield volcano
164 during the Late Miocene (Anjos Complex); 3) subsequent erosion and possible total
165 submersion producing heterogeneous volcanoclastic deposits, with synchronous low-
166 volume submarine lava effusions on the eastern side of the island during the Late
167 Miocene/Early Pliocene (Touril Complex); 4) increase in volcanic activity with a
168 gradual shift from submarine to subaerial eruptions, forming lava deltas along coeval
169 coastlines – and emergence of an elongated NNW-SSE-trending edifice during the
170 Early Pliocene (Facho-Pico Alto Complex); 5) subaerial and littoral erosion followed by
171 low-volume volcanism, forming a sequence of monogenetic cinder cones, during the
172 Late Pliocene (Feteiras Formation); and 6) uplift and erosion of the edifice from Early
173 Pleistocene to the present.

174

175

176 **3. Materials and methods**

177 *3.1. Sedimentological, taphonomical and palaeoecological analysis*

178 The outcrop at Pedra-que-pica was studied in detail to understand its overall
179 structure, geometry and field relationships between the sedimentary deposit and the

180 underlying and overlying volcanic sequences. A general geomorphological survey of
181 the local palaeotopography was conducted in order to assess the physical setting in
182 which the coquina was trapped. Special care was taken to record the lateral and vertical
183 facies changes, the sedimentary structures, the spatial disposition of the fossils, and the
184 position, identification, and taphonomical aspects of trace fossils. Data were collected
185 with the objective of constructing detailed cross sections and stratigraphic columns.
186 Fossils and bulk rock samples for micropalaeontological study were collected.
187 Macrofossils were photographed in the field, measured, and classified to genus and
188 species level whenever possible. Eight randomly selected quadrats of 1 m² were placed
189 on horizontal surfaces of the outcrop and all fossils within the quadrat were identified
190 and counted; taphonomic parameters (articulation of the valves, degree of
191 fragmentation, bioerosion signs and encrustations) were measured for 164 shells. The
192 outcrop was exhaustively surveyed for *Gigantopecten latissimus* (Brocchi, 1814), a
193 large bivalve mollusc that may reach a maximum length of ≈25 cm. All exposed
194 specimens of this species were counted and their shell settlement position (concave
195 up/down, oblique/vertical position) was recorded, as well as the articulation state of the
196 valves (articulated/disarticulated).

197 Because part of the coquina is presently underwater, the actual size of the outcrop
198 was examined by SCUBA diving. The sublittoral rocky substrate east of the presently
199 exposed area of the outcrop was surveyed and samples were collected and later
200 examined for the presence of carbonate sediments. From the exposed area of the
201 outcrop, representative samples of all main subunits of the deposit were collected for
202 petrographic investigations to identify structures, micro textures, mineralogy, and
203 microfossil content.

204 In compliance with the legislation of the Regional Government of the Azores, all
205 fossil specimens collected during this study were deposited in the Fossil Collection at
206 the Department of Biology of the University of the Azores (DBUA-F).

207

208 **4. Results**

209 *4.1. Geomorphology of pre-existing topography*

210 A prominent spur system composed of massive pillow lavas projects seaward
211 perpendicular from the shore, now subaerially exposed over a distance of 115 m
212 adjacent to the western edge of the Pedra-que-pica outcrop (Fig. 3). The existing spur
213 system attains a maximum elevation of 9 m above present sea level (apsl) on its western
214 side (2nd rocky spur of Fig. 3A, B), and is flanked by an irregular surface contiguous to
215 the east, eroded in the pillow lavas (1st rocky spur of Fig. 3A, B); the sedimentary
216 sequence rests unconformably on this surface and abuts against the 1st rocky spur to the
217 west. The unconformity between the eroded pillows and the overlying sediments is
218 exposed within the present-day tidal range, being visible around the margins of the
219 coquina outcrop and at several openings (blow holes) formed by wave erosion.

220

221 *4.2. Facies description, stratigraphy and sedimentological structures*

222 *4.2.1. Pliocene sedimentary succession*

223 The main outcrop at Pedra-que-pica consists of a 10 to 11 m thick succession of
224 marine fossiliferous sediments, of which only the uppermost 3 to 4 m are presently
225 exposed above sea level. These sediments are intercalated between an underlying
226 volcanic sequence and an overlying volcano-sedimentary sequence (Fig. 4A, B). The
227 base of the section is formed by pillow lavas (facies 1) which are truncated by an
228 erosional surface dipping towards ENE down to a depth of 6–7 m below mean sea-level

229 (bmsl). Locally, limited remains of strata that predate the coquina can be found in
230 spaces in between the pillow lavas, forming sandstone pockets composed of fine-
231 grained, light grey calcarenites (facies 2; Fig. 5). These calcarenites occupy a corner of
232 the eroded lava platform at its junction with the rocky spur system. Larger somatofossils
233 are absent from the calcarenites, but trace fossils belonging to *Macaronichnus*
234 *segregatis* Clifton and Thompson, 1978 are abundant (Figs. 3A, 6A, B), with rare
235 ?*Ophiomorpha* isp. (misidentified as *Thalassinoides* isp. by Kirby et al., 2007). Pockets
236 of calcareous sand among the pillow structures above this level and located on the
237 flanks of the spur system at a present height of 9 m amsl (white stars in Fig. 3A) also
238 feature additional examples of *M. segregatis*. Thin neptunian dikes filled with
239 calcareous sand are a prominent feature across the spur adjacent to the fossiliferous
240 sediments. *M. segregatis* occupies the sediments in these dikes, which can be traced
241 through a continuous vertical distance of 4 m (Fig. 6C, D). The calcarenite (facies 2;
242 Fig. 5) is unconformably truncated by an irregular erosion surface and covered by a 3-4
243 m thick unstructured coquina (facies 3a-c; Figs. 5, 7A-E, 8A, B).

244 The lower part of the coquina is submerged below present-day sea level. By scuba-
245 diving, we estimated its total area to be 23,463 m² (continuous hard white line in Fig.
246 3A). The intermediate part of the sequence is exposed at the intertidal zone as a shore
247 platform, extending for 3,179 m², whereas the upper part extends below the slope
248 deposits at the base of the present seacliff (Fig. 4A, B). The top of the coquina may be
249 traced laterally to a position near the adjacent spur (cf. Fig. 3), where it abuts against the
250 ravinement cut into the underlying calcarenites. About 1.0 m above the base of the
251 coquina it is possible to observe a 30 to 60 cm thick, discontinuous bed of subangular to
252 subrounded volcanic cobbles and boulders (facies 3b; Figs. 5, 7A, D), followed by
253 another unstructured, massive layer of coquina up to 2.6 m thick (facies 3c; Fig. 5). The

254 very poorly-sorted coquina-rudstone layers (facies 3a and 3c; Fig. 9A, B) are rich in
255 large, disarticulated bivalves (dominated by ostreids, pectinids and spondylids). It also
256 contains fewer echinoids (Fig. 8C), barnacles, brachiopods, bryozoans, calcareous algae
257 (rhodoliths) and small stony-corals. Teeth of bony fishes and sharks as well as moulds
258 of large gastropods (*Persististrombus* sp.) are rare, while whale bones are extremely
259 rare. The matrix of the coquina is predominantly composed of moderately sorted, sand-
260 size skeletal bioclasts (fragments of bivalves, echinoids, coralline algae, bryozoans as
261 well as benthic and planktonic foraminifers) with a smaller percentage of well-rounded
262 volcaniclasts (coarse palagonitic ash and tachylitic to lithic clasts) cemented by sparry
263 calcite (Fig. 9C, D).

264 Close to the top, the coquina contains rhodoliths (Fig. 8D) and abundant bryoliths
265 (i.e., nodules composed of bryozoans; Fig. 8E), as well as colonies of bryozoans with an
266 erect rigid growth form; these can be found within a fining upward to faintly bedded
267 calcarenite devoid of large clasts (facies 3d; Figs. 5, 8F). These calcarenites are ≈ 10 to
268 60 cm thick, show a sub-horizontal, very regular top, and are partly bioturbated
269 throughout the deposit. The most common trace fossil is *Asterosoma* isp., composed of
270 a cluster of concentrically layered spindle-shaped tubes, which diverge radially upward
271 from a common stem (Fig. 8G). Less common is a tubular backfill structure with a
272 central rod, ascribed to *Bichordites* isp., which occurs in the eastern part of the outcrop,
273 within the upper 1 to 2 cm of the calcarenite (Fig. 8H). The topmost 10 cm contain
274 abundant spines of the echinoid *Eucidaris tribuloides* (Lamarck, 1816) and fragments of
275 the coral *Porites* sp. The top of the calcarenite is locally scoured and some trace fossils
276 are truncated.

277 Abruptly overlying the bioturbated calcarenite (facies 3d) there follows a ≈ 36 m
278 thick unit of well-stratified, fine- to coarse-grained, vitric ash tuffs (facies 4a; Figs. 4,

279 10A; Kirby et al., 2007). The boundary between the two units is sharp. The basal 20–30
280 cm of the tuffs are characterized by relatively fine grain-sizes (fine ash) and by the
281 presence of water-escape structures (Fig. 10B). None of these structures appear to
282 penetrate the underlying calcarenites. Likewise, none of the calcarenite material is
283 incorporated in the basal tuff layers. Tuffitic material, however, infills the bioturbation
284 canaliculated conducts opened on the top of the calcarenite.

285 Sedimentary structures within the tuffs include thin planar lamination to medium-
286 thick bedding, low-angle cross-bedding, internal erosional surfaces where the planar
287 bedding is discordant and multiple reverse and normal graded beds. The tuff is a matrix-
288 supported fine-grained ash, locally palagonitised and cemented by micro zeolites. Clasts
289 are quite variable in size (0.25–2.5 mm) and consist of moderately rounded and
290 weathered lava clasts, and angular fragments and euhedral loose crystals (plagioclases,
291 olivines and clinopyroxenes). Fractures are cemented by secondary calcite (sparite)
292 (Fig. 9E). A single external mould of a bivalve (5.5 cm in length) was found within the
293 tuff, circa 20 cm above the contact with the calcarenite (Fig. 10C). Very rare angular
294 lava clasts (10–15 cm in size), are scattered within this unit (Fig. 10D). In addition to
295 these clasts of volcanic origin, a subordinate amount of lithic clasts (2–20 cm) of
296 sedimentary rock (Fig. 9F–H) are present within the tuffs. These clasts are represented
297 by a variety of different lithologies, ranging from bioclastic tuffaceous sandstone to
298 almost pure limestone (grainstone or rudstone with sparitic cement with a subordinate
299 amount of volcanoclastic fragments).

300 The tuffs are overlain by a <0.5 m thick conglomerate horizon (facies 4b; Fig. 4B)
301 that is followed by a thick lava-delta sequence composed of foresets of pillow lavas and
302 hyaloclastites (facies 4c) and a topset of flat-lying subaerial flows (facies 4d). The
303 passage zone between the subaerial and submarine flows marks the coeval sea level and

304 is nowadays located ≈ 50 m a.s.l. Towards the top of the cliff, the sequence is mostly
305 effusive and subaerial with the exception of occasional surtseyan tuff layers (facies 4e
306 and 4g), and a small set of submarine lava flows (facies 4f; Fig. 4B).

307

308 4.2.2. Pleistocene sedimentary succession

309 At the section locality (Fig. 4A, B), the tuffaceous sequence (facies 4a) is truncated
310 by a Pleistocene (MIS 5e; Ávila et al., 2008b, 2015) shore platform that reduced its
311 thickness to ≈ 4 m. The erosional unconformity and the overlying 0.5 to 1 m thick
312 boulder beach conglomerate (facies 5; Figs. 4B, 5) ends against a visible shore angle,
313 which is exposed ≈ 50 m to the east (Fig. 4B). The conglomerate is topped by a >20 m
314 thick, wedge-shaped terrigenous talus deposit (colluvium), consisting predominantly of
315 boulder breccias (facies 6; Figs. 4B, 5).

316

317 4.3. Palaeoecology and taphonomy of the coquina layers

318 The vast majority of the macrofossils in the coquina (facies 3a and 3c; Fig. 5) consist
319 of bivalve molluscs: *Chlamys hartungi* (Mayer, 1864), *Talochlamys abscondita* (Fischer
320 in Locard, 1898) [= *Hinnites ercolanianus* (Cocconi, 1873)], *Aequipecten opercularis*
321 (Linnaeus, 1758), *Pecten dunkeri* Mayer, 1864, *Argopecten* cf. *levicostatus* Toula, 1909
322 [= *Pecten* cf. *laevicostatus* (Soweby, 1844)], *Manupecten pesfelis* (Linnaeus, 1758),
323 *Gigantopecten latissimus* (Brocchi, 1814), *Arca noae* Linnaeus, 1758, *Anadara* sp.,
324 *Cubitostrea frondosa* (de Serres, 1829) [= *Ostrea frondosa* de Serres, 1829], *Ostrea* cf.
325 *edulis* Linnaeus, 1758 [= *O.* cf. *lamellosa* Brocchi, 1814], *Lopha plicatuloides* (Mayer,
326 1864), *Spondylus gaederopus* Linnaeus, 1758, *Spondylus* cf. *concentricus* Bronn, 1831,
327 and the boring bivalve *Myoforceps aristatus* (Dillwyn, 1817).

328 The results of surface-abundance counts on eight 1-m² quadrats show that *Ostrea*
329 spp. are the dominant species, ranging from 69 to 89%, with *Spondylus* spp. (4–9%),
330 *Manupecten pesfelis* (1–6%), *Chlamys hartungi* (1–9%), *Pecten dunkeri* (1–4%) and the
331 endemic *Lopha plicatuloides* (2–6%) as accessory species; *Gigantopecten latissimus*
332 ranges from 0 to 2%. Fossils of aragonitic gastropods and bivalves are nearly absent
333 from Pedra-que-pica, probably due to the preferential dissolution of aragonitic shells
334 during diagenesis (Valentine *et al.*, 2006). The only exceptions are a few poorly
335 preserved moulds of *Persististrombus* sp., *Conus* sp. and *Cheilea equestris* (Linnaeus,
336 1758).

337 In total, 70 different taxa could be determined: 38 bryozoans, 18 species of molluscs
338 (15 bivalves and 3 gastropods), 6 echinoids, 3 gnathostomata (two sharks and one
339 teleost), 2 balanid crustaceans, 1 brachiopod, 1 cnidarian and 1 mammal (an
340 unidentified whale) (Table 1).

341 Throughout the coquina, the majority of the larger pectinid shells (e.g.,
342 *Gigantopecten* longer than 10 cm) are concordant, lodged in a stable concave-down
343 position. The analysis of all the valves of *G. latissimus* visible on the coquina surface
344 (394 specimens) found that 389 were single disarticulated valves (98.7%) and only five
345 shells were still articulated (1.3%). Of the disarticulated shells, 347 valves were
346 concordant (286 in a stable concave-down position and 61 showed a concave-up
347 orientation), 25 were obliquely oriented – 15 of which with the concavity downwards
348 (3.8%) and 10 with the concavity upwards (2.5%) – and 17 were perpendicular (that is,
349 in a vertical position – 4.3%). Of the five articulated shells, three were preserved in a
350 concordant position (0.8%) and two in a perpendicular position (0.5%).

351 The orientation of the smaller bivalves, mainly composed by ostreids having all
352 valves disarticulated, was studied along three vertical profiles each 25 cm wide and 1.75

353 m, 2.50 and 2.75 m in height, respectively (Fig. 11A–C). A total of 1,482 ostreid shells
354 were counted, and their angles measured. The resulting rose diagrams (Fig. 11A–C)
355 demonstrate the main differences in the chaotic disposition of the smaller ostreids, with
356 most shells in concordant – either stable (concave-down) or unstable (concave-up)
357 (horizontal/sub-horizontal) – positions but with somewhat lesser numbers of valves in
358 perpendicular (vertical/subvertical) positions. In contrast, the large *Gigantopecten* (389
359 valves analysed) are predominantly in concordant (stable horizontal/subhorizontal)
360 positions (Fig. 11D). A further representative sample of 164 bivalves dominated by
361 *Ostrea* spp. (51.2%) and with subordinate amounts of *Lopha plicatuloides* (12.8%),
362 *Chlamys* spp (10.4%), *Spondylus* spp. (8.5%), *Pecten dunkeri* (7.3%), *Gigantopecten*
363 *latissimus* (4.9%), *Manupecten pesfelis* (4.3%) and *Arca noae* (0.6%) was examined for
364 taphonomical traits. All shells are disarticulated (100%, n= 164), 76.8% are fragmented
365 mostly on the edges (either on the umbo, dorsal or ventral margins), 68.9% show signs
366 of bioerosion and 82.3% have encrustations. Most bivalve shells are heavily bioeroded
367 on the external side of the valves (mostly *Gastrochaenolites* isp. produced by bivalves,
368 *Entobia* isp. by clionaid sponges, and *Caulostrepsis* isp. by spionid polychaetes), and
369 are commonly encrusted by bryozoans, balanids, oysters, serpulids and calcareous red
370 algae (listed in order of decreasing abundance). Despite this, they are generally well
371 preserved, with fragile skeletal elements still present (e.g., external ornamentation of
372 bivalves). Similarly, the tests of delicate echinoderms such as *Echinoneus* cf.
373 *cyclostomus* Leske, 1778 are also well preserved (Madeira et al., 2011).

374 The inner sides of most bivalves are usually encrusted by cheilostome and, to a lesser
375 degree, cyclostome bryozoans (cf. Table 1). Most, if not all, of these bryozoan species
376 are new to science and will be described elsewhere. The most ubiquitous bryozoan

377 species is *Onychocella* cf. *angulosa* (Reuss, 1847), which may cover large parts of or
378 even entire shells.

379

380

381 **5. Discussion**

382 *5.1. Palaeoenvironmental reconstructions*

383 Foremost consideration is given to the pre-existing topography. Similar to the present
384 day, it featured a prominent spur system, formed by pillow-lavas emplaced in latest
385 Miocene time that advanced to the south in a direction perpendicular to the present
386 shore (cf. Figs. 2, 3). An erosional platform was cut into the pillow-lava pile to form an
387 accumulation zone. Thereby, the spur system acted as an effective trap capable of
388 accommodating and retaining a considerable volume of bioclastic materials in the
389 littoral environment (Fig. 3A). This prominent coastal feature played a key role in
390 preventing the offshore transport of sediments, thus allowing accumulation of
391 sediments.

392 A lowering in sea level must have occurred after the emplacement of the submarine
393 lavas, because planation of the spur system's east flank took place under intertidal
394 conditions, incising a typical gently sloping (4°) shore platform where the coquina now
395 sits. Hence, the angle between the shore platform and the proximal spur, define a north-
396 south oriented palaeoshore that was subsequently drowned by a rise in sea level. The
397 original width of the eroded surface embraces the entire lava platform underneath the
398 adjacent coquina deposit, immediately to the east. The relief of the spur above the flat
399 platform now remains more than 9 m in height.

400 Remnants of the earliest phase of sedimentation covering the platform's shoreward
401 margin are represented by pockets of bioturbated calcarenite that include the trace fossil

402 *Macaronichnus segregatis* (Fig. 6A–D). Highly bioturbated sandstones with
403 *Macaronichnus* and mostly vertical, sparse crustacean burrows typically occur in upper
404 foreshore environments (e.g., Pemberton et al., 2001). Incipient *Macaronichnus* traces
405 are known to be produced today on sandy beaches by some ophelid polychaetes such as
406 those belonging to the genus *Euzonus* (Nara and Seike, 2004; Seike, 2007). Thus, mass
407 occurrences of this trace fossil are generally regarded as an excellent indicator of
408 intertidal to shallow subtidal conditions (i.e., upper foreshore). *Macaronichnus* isp. is
409 also recorded from shoreface settings in the Cape Verde Archipelago (Mayoral et al.,
410 2013; see also Bromley et al., 2009 for discussion of environmental range of
411 *Macaronichnus*), but as far as known, its occurrence within calcarenite sediments in
412 neptunian dikes such as the ones that dissect the spur adjacent to Pedra-que-pica is
413 unique (cf. Fig. 6C, D). The continuous representation of these fossil traces through a
414 vertical space of 4 m suggests a coeval sea-level rise. Moreover, as pockets of similar
415 carbonate sandstone are retained on the flanks of the parallel spur that is now 9 m a.s.l.,
416 it is inferred that a minimum change in local sea level amounted to at least 9 m during
417 the early stages of this succession. Therefore, we infer a coeval increase in water depth
418 above the adjacent coastal platform to become entirely subtidal. The fact that the
419 leading edge of the coquina partially truncates and cuts across the earlier calcarenites
420 (Fig. 6A), over a ravined morphology, is also interpreted as a result of this transgressive
421 regime.

422 The coquina appears to have been formed by at least three events, as indicated by the
423 occurrence of two shell beds (facies 3a and 3c), separated by a semi-continuous layer of
424 basaltic gravel (facies 3b; Figs. 5, 7D). This structure is interpreted to reflect discrete
425 pulses of material deposited under high-energy conditions, despite the lack of other
426 obvious internal stratification or structuring. A final resting place for this tri-part deposit

427 (shell bed, conglomerate, and shell bed) was effectively constrained by a natural
428 submarine configuration where the materials became trapped.

429 The abundant occurrence of bioeroded exterior and bryozoan-encrusted interior
430 valves of ostreids and pectinids argue for a primary (living bivalves) and secondary
431 origin (when post-mortem bioerosion and encrustation took place) of the Pedra-que-pica
432 coquina constituents, prior to final deposition. Whereas bioerosion primarily takes place
433 on upward-facing surfaces in the euphotic zone (Wisshak et al., 2010, 2011), most
434 bryozoans are cryptobionts and preferentially settle on the concave interior of shells,
435 which, in its energetically stable position, is facing downwards. In this way, boring
436 organisms and competition with fast growing photoautotrophs are avoided by the
437 bryozoan colonies (McKinney and Jackson, 1989; Wisshak et al., 2014). However, in
438 this outcrop, the bryozoan-encrusted concave side of many of the small ostreid and
439 pectinid valves face upward, which contrasts with the energetically stable position taken
440 by the majority of the large *Gigantopecten* valves (cf. Fig. 11). This bimodal
441 distribution occurs throughout the whole vertical section of the deposit, and thus must
442 be related to intrinsic characteristics of the process of deposition at this depth. The
443 bimodality might be explained by a debris fall sensu Titschack et al. (2005), with
444 different hydrodynamic behaviours of shells according to their size and shape. The
445 smaller and more convex shells (like the ostreids) might settle from suspension in the
446 concave-up position, exhibiting greater lift-to-drag ratio than the bigger and flatter
447 shells (like the *Gigantopecten*), and thus may be more prone to movement by rolling,
448 whereas the larger and flatter shells are transported by a sliding process along the slope
449 which might favour a deposition in more stable positions (see Oliveira and Wood,
450 1997). An alternative explanation is that bottom current velocities during storm events
451 were high enough to overturn the large and heavy recently deposited *Gigantopecten*

452 shells to their most stable position (concave-down) and that these high velocities
453 induced a chaotic deposition of the smaller and much more abundant ostreids shells,
454 which were quickly covered (and thus locked in unstable positions) by successive layers
455 of new shells. In detail, however, this deposition model needs to be refined and the
456 cause for the bimodality further investigated.

457 The trigger mechanism for such energetic depositional conditions is not entirely
458 clear. The coquina lacks most of the features diagnostic of (shelly) storm
459 beds/tempestites, such as grading and sole structures, as defined in Reineck and Singh
460 (1973) or Aigner (1987), possibly due to the coarse grain size. Earthquakes and storms
461 could be responsible for triggering these re-depositional events. Since earthquakes are
462 much less frequent than large storms in the region, storms are the most probable
463 initiators of the redeposition.

464 The fossil assemblages at Pedra-que-pica indicate a shallow-marine source: the
465 balanids *Zullobalanus santamariaensis* Buckeridge and Winkelmann, 2010 and the
466 bivalve *Gigantopecten latissimus* predominantly inhabited agitated shallow-water
467 environments (e.g., Bongrain, 1988; Harzhauser et al., 2003; Winkelmann et al., 2010);
468 rhodoliths require at least periodically prevailing high-energy conditions and the former
469 require habitats within the photic zone (Piller and Rasser, 1996); extant clypeasteroids
470 close to *Clypeaster altus* (Leske, 1778), as well as extant cidarids such as *Eucidaris*
471 *tribuloides* (Lamarck, 1816) are predominantly littoral inhabitants, being most common
472 above 50 m water depth (Madeira et al., 2011); *Myoforceps aristatus* is an extant boring
473 bivalve that lives in calcareous substrates commonly just below the low tide mark. This
474 bivalve does not occur in the Azores today due to the lack of appropriate substrate
475 (Ávila et al., 2010), as it is not able to bore lava and carbonate production is very
476 limited, but it was a very common species at Santa Maria during the formation of the

477 Pedra-que-pica deposit, boring rhodoliths and bryoliths, as well as bivalve shells. The
478 borings *Gastrochaenolites*, *Entobia* and *Caulostrepsis*, are typical members of the
479 *Entobia* ichnofacies, whose formation requires exposition of the substrate for months, if
480 not years (Bromley, 1992). These borings occur mostly in the deeper intertidal and
481 shallow subtidal zones (Ekdale et al., 1984), typically on upward-facing surfaces of
482 shells (Wisshak et al., 2010). Most fossils (especially the bivalve shells and their
483 encrusting bryozoans), exhibit a low degree of fragmentation (mostly limited to the
484 edges of the shell), abrasion and/or reworking, which – together with the poor sorting –
485 indicates a proximal provenance followed by transport and deposition of the coquina
486 into somewhat deeper waters below fair-weather wave base, where low-energy
487 conditions prevented further reworking and fragmentation of the shell material.
488 Therefore, the fossil assemblage at Pedra-que-pica represents an allochthonous fauna
489 generated at a highly productive carbonate factory at shallower levels, later transported
490 (as argued above) to a calmer, deeper depocenter.

491 The occurrence of just only five paired *Gigantopecten* valves (<1.3%), together with
492 the degree of shell fragmentation and sorting, also indicates a swift removal and rapid
493 transport of the shell accumulation from a nearby source. With the exception of
494 bioclasts of the stony coral *Porites* (which are mainly composed of aragonite), the lack
495 of other aragonitic bioclasts and the predominance of oysters, echinoids, pectinids,
496 barnacles, and other calcitic taxa in the coquina is interpreted as a taphonomical artefact
497 due to early diagenetic dissolution of shell aragonite prior to lithification.

498 In temperate latitudes, post-mortem disarticulation of pectinid shells due to the decay
499 of the organic ligaments occurs in a matter of months to years (Christmas et al., 1997;
500 Best, 2008). At the time of deposition, the palaeoclimatic conditions around Santa
501 Maria would have been typical of a tropical environment, thus the degradation of soft

502 tissues and the consequent disarticulation of the pectinid valves would have been faster
503 (weeks to months) than in a more temperate climate (Best et al., 2004). We infer
504 tropical sea-surface temperatures (SST's) based on the high frequency of the shallow
505 *Gigantopecten latissimus* and *Clypeaster altus*, as well as on the presence of
506 *Persististrombus* sp., *Ficus* sp., *Conus* spp., *Xenophora* sp. and *Porites* sp. The first
507 three taxa were the most important warm-water taxa of the “Mediterranean Plio-
508 Pleistocene Molluscan Unit 1” (Raffi and Monegatti, 1993; Monegatti and Raffi, 2001;
509 Landau et al., 2011), a Zanclean-mid Piacenzian ecostratigraphical unit based on
510 molluscs (Monegatti and Raffi, 2007). The common occurrence of specimens of
511 *Persististrombus* at Pedra-que-pica further points towards much higher SST's than the
512 present minimum sea-surface temperature in the Azores around 14°C in the winter
513 period (Wisshak et al., 2010). Indeed, according to several authors, the presence of
514 *Persististrombus* requires mean annual SST around 23–24°C, and winter SST not below
515 19–21°C (Bardají et al., 2009; Zazo et al., 2010). Thus, we infer that at the time of
516 deposition of the coquina at Pedra-que-pica, tropical conditions were prevalent, with
517 minimum sea-surface palaeotemperatures (at least) over 19°C, which is five degrees
518 higher than nowadays.

519 In summary, we interpret the fossiliferous sequence at Pedra-que-pica to represent a
520 succession of several debris-fall deposits (sensu Titschack et al., 2005) whose
521 redeposition was triggered by major storm events that removed the sediments from its
522 original nearshore setting (Fig. 12B) to a higher gradient area of the shelf. These events
523 brought shell materials to a local depocenter below fair-weather wave base (cf. Figs. 2,
524 12C), where the lava spur system acted like a protective coastal groin. The
525 accumulation of fine sediments continued during subsequent fair-weather conditions,
526 when the calcarenite at the top of the coquina was colonised by invertebrate settlers. As

527 a result, it shows increased bioturbation by polychaetes and large spatangoid echinoids,
528 which produced *Asterosoma* isp. and *Bichordites* isp., respectively (Fig. 12D; Uchman,
529 1995, 1998). *Asterosoma* and *Bichordites* can be ascribed to the impoverished
530 archetypal *Cruziana* ichnofacies, which is typical of shoreface-offshore transition and
531 upper offshore, below the fair-weather wave base (e.g., Pemberton et al., 2001). The
532 impoverishment can be caused by the shelly ground below the calcarenites, preventing
533 deep burrowing, and by small scale scouring before deposition of water-settled tuff,
534 which might erosionally remove some shallower burrows (see section 5.3).

535

536 5.3. Preservation of the deposit and subsequent events

537 The sharp transition between the calcarenite and overlying water-settled tuff (facies
538 4a, Fig. 4B; facies 4, Fig. 5) demonstrates an abrupt change in sediment supply, related
539 to the onset of a new volcanic phase in this area, probably from the Rocha Alta volcanic
540 cone, located ≈ 600 m to the west of Pedra-que-pica. Prior to this eruption, part of the
541 top of the calcarenite was removed, probably by a storm. This reasoning is based on the
542 *Bichordites* isp. (Fig. 8G) that was typically produced by spatangoid echinoderms,
543 usually at depths of 5 to 50 cm from the top of the sediment surface (Bromley *et al.*,
544 1997). As this ichnofossil is at a depth of only 1 to 2 cm from the contact between the
545 calcarenite and water-settled tuff, it is inferred that several centimetres of sediment were
546 removed. Rapid and voluminous accumulation of loose lapilli- to ash-sized pyroclastic
547 particles subsequently sealed the remaining sediments below, and thus favoured their
548 preservation.

549 Angular lithic clasts of marine sedimentary origin and isolated gastropods within the
550 water-settled tuffs (Fig. 9F–H) are classified as “accidental clasts” (cf. Fisher and
551 Schmincke, 1984) that were produced and became entrained by the disruption of pre-

552 existing, lithified country rocks at the seafloor during explosive hydromagmatic
553 eruptions. Their angular clast shapes indicate that such volcanoclastic calcarenites were
554 already lithified at the time of the eruption and that transportation distances were short.
555 Some clasts are composed of material similar to the matrix of the coquina and the
556 overlying calcarenite. Others, however, are very pure, well cemented limestone with
557 subordinate volcano-detritic content and abundant gastropods (cf. Fig. 8H), i.e.
558 aragonitic shells are preserved, which indicates that the source is different than that of
559 Pedra-que-pica, where aragonite was dissolved prior to lithification. The single external
560 mould of a bivalve (Fig. 10C) is also an “accidental clast”. It is interpreted as a shell
561 that, projected together with the pyroclasts, became entrained in the volcanic plume
562 from the sea floor, and was thus deposited together with the water-settled tuffs.

563 The absence of bioturbational structures, prominent unconformities, or larger
564 intercalations of epiclastic material within the tuffs indicates rapid deposition and a
565 continuous and voluminous supply of pyroclastic material in a relatively short period of
566 time. The massive provision of loose tuffaceous material caused the sedimentary system
567 to switch from retrogradational to progradational.

568 The deformed structures at the base of the tuffs are interpreted as fluid-escape
569 structures (Fig. 10B). They might be attributed to sediment liquefaction during
570 earthquakes, when localised fluid-escape velocities are higher than those needed for
571 minimum sediment fluidisation (Judd and Hoveland, 2007). Alternatively, they could be
572 indicative of an abrupt overburden, and thus a rapid deposition of the tuffs, which
573 caused the underlying, fluid-saturated sediment to dewater due to sedimentary overload.

574 The absence of ballistic emplacement structures of volcanic bombs and blocks (e.g.,
575 impact pits, bomb sags) suggests a submarine origin for these pyroclasts, classifying
576 them as water-settled surtseyan tuffs formed by hydromagmatic volcanic activity in

577 relatively shallow waters (Fisher and Schmincke, 1984). The subaquatic deposition of
578 the tuff layers is further corroborated by the common occurrence of cross-bedding and
579 small cross-cutting channels, as we interpret these sedimentary structures not as primary
580 structures typical of surge (diluted turbulent pyroclastic flow) deposits, common in
581 surtseyan eruptions (as they would be if subaerial and related to the deposition of the
582 tuffs), but as secondary structures related to the marine environment and the rapid
583 resedimentation of the tuffs.

584 At an elevation of ≈ 35 m amsl, the top of tuffaceous unit is overlain by a thin (<1 m)
585 conglomerate bed (facies 4b; Fig. 4B). The unconformity and the overlying
586 conglomerate indicate erosion and reworking in comparatively shallow water.
587 Following the formation of the conglomerate on top of the tuffs, another period of
588 volcanism emplaced the overlying lava delta (facies 4c and 4d; Fig. 4B). Low palaeo-
589 relief characterises the transition between the conglomerate and the submarine
590 volcanics, which indicates a short hiatus due to sediment reworking. Pillows and
591 palagonitised hyaloclastites constitute the basal part (facies 4c; Fig. 4B), indicating
592 submarine volcanism. The submarine lavas are topped by massive subaerial flows
593 (facies 4d; Fig. 4B), with the transition between submarine and subaerial environments
594 occurring at an altitude of ≈ 50 m amsl, marking very accurately the position of coeval
595 sea-level (Fig. 4B). Thus, the volcano-sedimentary sequence overlying the fossiliferous
596 sediments further attests to a sea-level rise of around 50 m.

597

598 *5.4. Sedimentation on the shelves of volcanic oceanic islands*

599 In the highly dynamic environment of volcanic oceanic islands, it is unusual to find
600 marine sediments preserved in bulk, although carbonate may be abundantly produced
601 by a range of benthic organisms in euphotic to aphotic conditions (Wisshak et al.,

602 2014). Island shelves in these settings are typically very narrow and steep, exposed to
603 high-wave energy and, thus, offer little accommodation space compared to continental
604 shelves (Ávila et al., 2008a; Quartau et al., 2010, 2012). Present-day submarine deposits
605 on such island shelves are affected by strong, offshore-directed, downwelling currents
606 that form to compensate coastal setup of storm surges (Tsutsui et al., 1987; Chiocci and
607 Romagnoli, 2004; Quartau et al., 2010, 2012, 2015; Meireles et al., 2013).

608 The typical morphology of these shelves and the exposure to high-energy conditions
609 are unfavourable for preservation of depositional sequences older than those dating
610 from the present highstand. As shorelines migrate downwards across the shelf during
611 sea-level drops, downwelling currents are more likely to transport sediments over the
612 shelf edge where they are ultimately lost to the deep-island slopes (Ávila et al., 2008a,
613 2010; Quartau et al., 2012). Occasionally, chances for preservation may be enhanced by
614 adequate geomorphological features (e.g. natural barriers, bays, channels, gullies,
615 depressions, etc.), sediment textures (coarse deposits) and lithification (Quartau et al.,
616 2012). However, the single most important contributor to preservation is volcanic
617 capping. Exposure, on the other hand, is only possible on islands that experience uplift
618 (or eventually vertical stability and sea-level fall). That is why other marine deposits
619 have been described from Atlantic islands such as Madeira, Porto Santo and Selvagens
620 (Mayer, 1864; Cotter, 1892; Gerber, 1989; Johnson et al., 2011; Santos et al., 2011;
621 Baarli et al., 2014; Ramalho et al., 2015), as well as the Canary (Zazo et al., 2002) and
622 Cape Verde archipelagos (Zazo et al., 2007, 2010; Ramalho et al., 2010; Ramalho,
623 2011; Johnson et al., 2012; Baarli et al., 2013). All these islands experienced uplift
624 episodes during their geological history, and sea-level fall relative to the Last
625 Interglacial period. Therefore, to find well-preserved shell accumulations on reefless

626 volcanic oceanic islands is unusual, as only a few experienced the necessary conditions
627 for preservation and exposure.

628 Additionally, massive fossil accumulations preferentially form when sedimentation is
629 reduced, i.e., during transgressions (Kidwell et al., 1986; Kidwell, 1991). However,
630 these condensed sections are less likely to be preserved in the geological record of
631 continental margins (Scarponi et al., 2013) and even less likely on insular shelves
632 (Ávila, 2008a; Quartau et al., 2012; Meireles et al., 2013). Fortunately, in volcanic
633 settings, eruptions may locally entomb marine deposits through rapid and abrupt burial,
634 thus locally preserving the transgressive sedimentary record. Consequently, volcanic
635 events have the potential to interrupt carbonate production but also provide the hard
636 substrata for a diverse benthic ecosystem and development of an offshore carbonate
637 factory in the first place (e.g. Wisshak et al., 2010). Volcanoes also can be responsible
638 for the effective preservation of marine deposits on oceanic-island shelves (cf. Meireles
639 et al., 2013).

640

641

642 **6. Conclusions**

643 The sedimentary deposits at Pedra-que-pica are the result of localised biotic and
644 abiotic factors that operated under a rare confluence of the following events:

- 645 1. Sea-surface temperatures above 19°C and sunlight worked to elevate
646 productivity in a nearshore shelf setting around Santa Maria Island, with the
647 resulting development of a shallow carbonate factory;
- 648 2. A natural coastal groin formed by a resistant spur of basalt perpendicular to the
649 island's south shore and adjacent to a shore platform where deposition was

650 already present in the Pliocene; the angle between the spur and the platform
651 demarks a palaeoshore;

652 3. The first depositional event on this shore platform was the accumulation of
653 carbonate sand in an intertidal to very shallow water setting. This depositional
654 depth is inferred by the presence of neptunian dikes filled with carbonate sand
655 that hosted intertidal organisms that left behind the trace fossil *Macaronichnus*
656 *segregatis*. The continuous migration of the trace maker in vertical dikes
657 reaching upward for 4 m represents a rise in relative sea level. The sea-level
658 continued to rise to a level deep enough to accommodate the next depositional
659 sequence (coquina);

660 4. Through a succession of no less than three debris-fall events initially triggered
661 by storms, the deepening accommodation space on the platform received a tri-
662 part accumulation of sediment that formed a shell coquina, a conglomerate, and
663 a second shell coquina;

664 5. The coquina deposit is formed by disarticulated bivalve shells (dominated by
665 *Ostrea* spp. as much as 89% by count), has an overall preserved thickness of
666 several meters (at least 11 m) and covers an uneven platform inferred to be over
667 23,400 m² in area;

668 6. The deposition of shells and other biological material occurred below fair-
669 weather wave base, where low-energy conditions prevented reworking and shell
670 fragmentation;

671 7. Erosion of the calcarenites on top of the coquina took place prior to
672 emplacement of the water-settled tuffs, which were capped by a lava delta
673 sequence that effectively sealed the fossiliferous succession from any further
674 disturbance until its relatively recent exhumation due to uplift and erosion.

675

676 This study contributes to the understanding of processes responsible for the transport
677 and sedimentation on the shelves that surround reefless volcanic oceanic islands. It also
678 highlights the importance of the Pedra-que-pica coquina within an oceanic island
679 context, because very special conditions are required for the preservation and exposure
680 of similar deposits on shelf environments of reefless volcanic oceanic islands. The same
681 exciting avenue of research may be advanced by similar studies in other archipelagos.
682 Finally, the extreme rarity and hence the international interest in this deposit calls for a
683 reinforcement of its legal protection and continuation of further studies at Pedra-que-
684 pica.

685

686

687 **Acknowledgements**

688 Comments and suggestions from the editor Finn Surlyk, Anne Mehlin Sørensen
689 (University of Copenhagen) and from an anonymous reviewer were greatly appreciated
690 and helped to significantly improve this manuscript. We thank the Direcção Regional da
691 Ciência, Tecnologia e Comunicações (Regional Government of the Azores), FCT
692 (Fundação para a Ciência e a Tecnologia) of the Portuguese Government, and Câmara
693 Municipal de Vila do Porto for financial support; the Clube Naval de Santa Maria and
694 Câmara Municipal de Vila do Porto for field assistance. We also acknowledge the
695 Direcção de Serviços de Cartografia e Informação Geográfica for providing GIS
696 topographic mapping of Santa Maria Island. We thank Eduardo Mayoral (University of
697 Huelva) for helping on the identification of the ichnofossils at an early stage of the
698 study. We are grateful to the organizers and participants of several editions of the
699 International Workshop “Palaeontology in Atlantic Islands” who helped in fieldwork

700 (2002–2014). Ricardo Ramalho’s funding was provided by DFG-The German Research
701 Foundation, through the project “Investigation of ocean island uplift in the Azores
702 Island Region”. Ana Cristina Rebelo, Patrícia Madeira, Ricardo Cordeiro, Ricardo
703 Piazza Meireles and Ana Hipólito benefited, respectively, from grants
704 SFRH/BD/77310/2011, SFRH/BD/61146/2009, SFRH/BD/60366/2009,
705 SFRH/BD/60518/2009 and SFRH/BD/73664/2010 by FCT, Portugal. Vittorio Zanon
706 was funded by DRCT through grant M3.1.7/F/008A/2009 (Portugal). Sérgio Ávila and
707 Rui Quartau acknowledge their Ciência 2008 research contracts funded by FCT. Mario
708 Cachão (calcareous nannoplankton) benefited from project Cd-ToxCoN FCT
709 (PTDC/MAR/102800/2008). Jörg Habermann and Jürgen Titschack were funded by
710 DFG (Project BE4459/1-1). This research also received substantial support from the
711 SYNTHESYS Project (<http://www.synthesys.info/>), which is financed by the European
712 Community Research Infrastructure Action under the FP7 “Capacities” Program; Sérgio
713 Ávila studied fossil molluscs at the Museum für Naturkunde, Berlin (DE-TAF-1071),
714 while Björn Berning visited the Museum National d'Histoire Naturelle Paris (FR-TAF-
715 1902) and the Natural History Museum London (GB-TAF-3347) to study bryozoan type
716 material.

717

718

719 **References**

720 Abdel-Monem, A.A., Fernandez, L.A., Boone, G.M., 1975. K-Ar ages from the eastern
721 Azores group (Santa Maria, São Miguel and the Formigas Islands). *Lithos* 8,
722 247–254, doi: 10.1016/0024-4937(75)90008-0.

723 Aguirre, J., 1995. Implicaciones estratigráficas y paleogeográficas de dos
724 discontinuidades estratigráficas en los depósitos pliocenos de Cádiz (SW de
725 España). *Revista de la Sociedad Geológica de España* 8, 153–166.

726 Aigner, T., 1987. *Storm Depositional Systems: Dynamic Stratigraphy in Modern and*
727 *Ancient Shallow-Marine Sequences. Lecture Notes in Earth Sciences*, Springer
728 Verlag, Berlin.

729 Ávila, S.P., 2013. Unravelling the patterns and processes of evolution of marine life in
730 oceanic islands: a global framework. In: Fernandez-Palacios, J.M. (ed.),
731 *Climate Change: Past, Present and Future Perspectives. A Global Synthesis*
732 *from the Atlantic. Universidad de La Laguna, Tenerife*, 95–125.

733 Ávila, S.P., Amen, R., Azevedo, J.M.N., Cachão, M., García-Talavera, F., 2002.
734 Checklist of the Pleistocene marine molluscs of Prainha and Lagoinhas (Santa
735 Maria Island, Azores). *Açoreana* 9, 343–370.

736 Ávila, S.P., Madeira, P., da Silva, C.M., Cachão, M., Quartau, R., Martins, A.M.F.,
737 2008a. Local disappearance of bivalves in the Azores during the last glaciation.
738 *Journal of Quaternary Science* 23, 777–785. doi: 10.1002/jqs.1165.

739 Ávila, S.P., Madeira, P., Mendes, N., Rebelo, A., Medeiros, A., Gomes, C., García-
740 Talavera, F., Silva, C.M. da, Cachão, M., Hillaire-Marcel, C., Martins, A.M.F.,
741 2008b. Mass extinctions in the Azores during the last glaciation: fact or myth?
742 *Journal of Biogeography* 35, 1123–1129. doi: 10.1111/j.1365-
743 2699.2008.01881.

744 Ávila, S.P., da Silva, C.M., Schiebel, R., Cecca, F., Backeljau, T., Martins, A.M.F.,
745 2009a. How did they get here? Palaeobiogeography of the Pleistocene marine
746 molluscs of the Azores. *Bulletin of the Geological Society of France* 180(4),
747 295–307. doi: 10.2113/gssgfbull.180.4.295.

748 Ávila, S.P., Madeira, P., Zazo, C., Kroh, A., Kirby, M., da Silva, C.M., Cachão, M.,
749 Martins, A.M.F., 2009b. Palaeoecology of the Pleistocene (MIS 5.5) outcrops
750 of Santa Maria Island (Azores) in a complex oceanic tectonic setting.
751 Palaeogeography, Palaeoclimatology, Palaeoecology 274(1–2), 18–31. doi:
752 10.1016/j.palaeo.2008.12.014.

753 Ávila, S.P., Rebelo, A., Medeiros, A., Melo, C., Gomes, C., Bagaço, L., Madeira, P.,
754 Borges, P.A., Monteiro, P., Cordeiro, R., Meireles R., Ramalho, R., 2010. Os
755 fósseis de Santa Maria (Açores). 1. A jazida da Prainha. OVGA – Observatório
756 Vulcanológico e Geotérmico dos Açores, Lagoa, pp. 1–103.

757 Ávila, S.P., Ramalho, R., Vullo, R., 2012. Systematics, palaeoecology and
758 palaeobiogeography of the Neogene fossil sharks from the Azores (Northeast
759 Atlantic). *Annales de Paléontologie* 98(3), 167–189. doi:
760 10.1016/j.annpal.2012.04.001.

761 Ávila, S.P., Melo, C., Silva, L., Ramalho, R., Quartau, R., Hipólito, A., Cordeiro, R.,
762 Rebelo, A.C., Madeira, P., Rovere, A., Hearty, P.J., Henriques, D., Silva, C.M.
763 da, Martins, A.M.F., Zazo, C., 2015. A review of the MIS 5e highstand
764 deposits from Santa Maria Island (Azores, NE Atlantic): palaeobiodiversity,
765 palaeoecology and palaeobiogeography. *Quaternary Science Reviews* 114,
766 126–148.

767 Baarli, B.G., Santos, A., Mayoral, E., Ledesma-Vázquez, J., Johnson, M.E., da Silva,
768 C.M., Cachão, M., 2013. What Darwin did not see: Pleistocene fossil
769 assemblages on a high-energy coast at Ponta das Bicudas, Santiago, Cape
770 Verde Islands. *Geological Magazine* 150(1), 183–189. doi:
771 10.1017/S001675681200074X.

- 772 Baarli, B.G., Cachão, M., da Silva, C.M., Johnson, M.E., Mayoral, E., Santos, A., 2014.
773 A Middle Miocene carbonate embankment on an active volcanic slope: Ilhéu
774 de Baixo, Madeira Archipelago, Eastern Atlantic. *Geological Journal*. First
775 published online 05, 2013. doi: 10.1002/gj.2513.
- 776 Bardají, T., Goy, J.L., Zazo, C., Hillaire-Marcel, C., Dabrio, C.J., Cabero, A., Ghaleb,
777 B., Silva P.G., Lario, J., 2009. Sea level and climate changes during OIS 5e in
778 the Western Mediterranean. *Geomorphology* 104, 22–37.
- 779 Beier, C., Mata, J., Stöckhert, F., Mattielli, N., Brandl, P.A., Madureira, P., Genske,
780 F.S., Martins, S., Madeira, J., Haase, K.M., 2012. Geochemical evidence for
781 melting of carbonated peridotite on Santa Maria Island, Azores. *Contributions*
782 *to Mineralogy and Petrology* 165(5), 823–841. doi: 10.1007/s00410-012-0837-
783 2.
- 784 Best, M.M.R., Burniaux, P., Pandolfi, J.M., 2004. Experimental bivalve taphonomy in
785 reefs of Madang Lagoon, Papua New Guinea. In: Best, M.M.R. and Caron, J.-
786 B. (eds.), *Canadian Paleontology Conference Proceedings No. 2*. Geological
787 Association of Canada Publications, St. John's, 8–12.
- 788 Best, M.M.R., 2008. Contrast in preservation of bivalve death assemblages in
789 siliciclastic and carbonate tropical shelf settings. *Palaios* 23, 796–809. doi:
790 10.2110/palo.2005.p05-076r.
- 791 Bongrain, M., 1988. *Les Gigantopecten (Pectinidae, Bivalvia) du Miocène Français*.
792 *Cahiers de Paleontologie*, Édition du Centre National de la Recherche
793 Scientifique, Paris, pp 1–230.
- 794 Bromley, R.G., 1992. Bioerosion: eating rocks for fun and profit. In: Maples, C. and
795 West, R.R. (eds.), *Trace Fossils. Short Courses in Paleontology* 5, 121–129.

796 Bromley, R.G., Asgaard, U., Jensen, M., 1997. Experimental study of sediment
797 structures created by a spatangoid echinoid, *Echinocardium mediterraneum*.
798 Proceedings of the Geologists' Association 108(3), 183–189. doi:
799 10.1016/S0016-7878(97)80026-0.

800 Bromley, R.G., Uchman, A., Milàn, J. Hansen, K.S., 2009. Rheotactic *Macaronichnus*,
801 and human and cattle trackways in Holocene beachrock, Greece: reconstruction
802 of palaeoshoreline orientation. *Ichnos* 16(1–2), 103–117.

803 Cannat, M., Briais, A., Deplus, C., Escartín, J., Georgen, J. L., Mercouriev, S., Meyzen,
804 C., Muller, M., Pouliquen, G., Rabain, A., Silva, P., 1999. Mid-Atlantic Ridge
805 – Azores hotspot interactions: along-axis migration of a hotspot-derived event
806 of enhanced magmatism 10 to 4 Ma ago. *Earth and Planetary Science Letters*
807 173, 257–269.

808 Chiocci, F.L., Romagnoli, C., 2004. Submerged depositional terraces in the Aeolian
809 Islands (Sicily). In: Chiocci, F.L., D'Angelo, S. and Romagnoli, C. (eds.),
810 Atlas of submerged depositional terraces along the Italian coasts. *Descriptive*
811 *Memories of the Geological Map of Italy* 58, 81–114.

812 Christmas, J.F., McGinty, M.R., Randle, D.A., Smith, G.F., Jordan, S.J., 1997. Oyster
813 shell disarticulation in three Chesapeake Bay tributaries. *Journal of Shellfish*
814 *Research* 16(1), 115–123.

815 Cotter, J.C.B., 1892. Notícia de alguns fósseis terciários do Archipelago da Madeira.
816 *Comunicações da Comissão dos Trabalhos Geológicos de Portugal* 2(2), 1–19.

817 Crook, K.A.W., Felton, E.A., 2008. Sedimentology of rocky shorelines 5: The marine
818 samples at +326 m from 'Stearns swale' (Lanai, Hawai'i) and their
819 paleoenvironmental and sedimentary process implications. *Sedimentary*
820 *Geology* 206, 33–41. doi: 10.1016/j.sedgeo.2008.02.007.

821 Donovan, S.K., 2002. Island shelves, downslope transport and shell assemblages.
822 *Lethaia* 35(3), 277, doi: 10.1111/j.1502-3931.2002.tb00086.x.

823 Ekdale, A.A., Bromley, R.G., Pemberton, G.S., 1984. *Ichnology: The Use of Trace*
824 *Fossils in Sedimentology and Stratigraphy*. Society of Economic Geologists
825 and Paleontologists, Short Course, 15, 1-317.

826 Esteves, M., Ávila, S.P., 2007. Fossil whales from the Azores. In: Ávila, S.P. and de
827 Frias Martins, A.M. (eds.), *Proceedings of the 1st Atlantic Islands Neogene*.
828 *Açoreana Suplemento 5*, 140–161.

829 Fallaw, W.C., 1973. Depositional environments of marine Pleistocene deposits in
830 southeastern North Carolina. *Bulletin of the Geological Society of America*
831 84(1), 257–268, doi: 10.1130/0016-7606(1973)84<257:DEOMPD>2.0.CO;2.

832 Felton, E.A., Crook, K.A.W., Keating, B.H., Kay, E.A., 2006. Sedimentology of rocky
833 shorelines: 4. Coarse gravel lithofacies, molluscan biofacies, and the
834 stratigraphic and eustatic records in the type area of the Pleistocene Hulopoe
835 Gravel, Lanai, Hawaii. *Sedimentary Geology* 184(1–2), 1–76, doi:
836 10.1016/j.sedgeo.2005.08.005.

837 Ferreira, O.V., 1955. A fauna Miocénica da ilha de Santa Maria. *Comunicações dos*
838 *Serviços Geológicos de Portugal* 36, 9–44.

839 Fisher, R.V., Schmincke, H.-U., 1984. *Pyroclastic Rocks*. Springer-Verlag, Berlin, 427
840 pp.

841 Gente, P., Dymant, J., Maia, M., Goslin, J., 2003. Interaction between the Mid-Atlantic
842 Ridge and the Azores hot spot during the last 85 Myr: Emplacement and rifting
843 of the hot spot-derived plateaus. *Geochemistry, Geophysics, Geosystems* 4(10),
844 8514–8537, doi: 10.1029/2003GC000527.

845 Gerber, J., Hemmen, J., Groh, K., 1989. Eine pleistozäne marine Molluskenfauna von
846 Porto Santo (Madeira-Archipel). *Mitteilungen der Deutschen*
847 *Malakozoologischen Gesellschaft* 44–45, 19–30.

848 Harzhauser, M., Mandic, O., Zuschin, M., 2003. Changes in Paratethyan marine
849 molluscs at the Early/Middle Miocene transition: diversity, palaeogeography
850 and palaeoclimate. *Acta Geologica Polonica* 53(4), 323–339.

851 Janssen, A.W., Kroh, A., Ávila, S.P., 2008. Early Pliocene heteropods and pteropods
852 (Mollusca, Gastropoda) from Santa Maria Island (Azores, Portugal):
853 systematics and biostratigraphic implications. *Acta Geologica Polonica* 58(3),
854 355–369.

855 Johnson, M.E., Silva, C.M. da, Santos, A., Baarli, B.G., Cachão, M., Mayoral, E.,
856 Rebelo, A.C., Ledesma-Vázquez, J., 2011. Rhodolith transport and
857 immobilization on a volcanically active rocky shore: Middle Miocene at
858 Cabeço das Laranjas on Ilhéu de Cima (Madeira Archipelago, Portugal).
859 *Palaeogeography, Palaeoclimatology, Palaeoecology* 300(1–4), 113–127, doi:
860 10.1016/j.palaeo.2010.12.014.

861 Johnson, M.E., Baarli, B.G., Cachão, M., Silva, C.M. da, Ledesma-Vásquez, J.,
862 Mayoral, E., Ramalho, R.S., Santos, A., 2012. Rhodoliths, uniformitarianism,
863 and Darwin: Pleistocene and Recent carbonate deposits in the Cape Verde and
864 Canary archipelagos. *Palaeogeography, Palaeoclimatology, Palaeoecology*
865 329–330, 83–100, doi: 10.1016/j.palaeo.2012.02.019.

866 Judd, A., Hoveland, M., 2007. *Seabed Fluid Flow: the Impact of Geology, Biology and*
867 *the Marine Environment*. Cambridge University Press, Cambridge, 475 pp.

868 Kidwell, S.M., Fürsich, F.T., Aigner, T., 1986. Conceptual framework for the analysis
869 and classification of fossil concentrations. *Palaaios* 1, 228–238.

870 Kidwell, S.M., 1991. The stratigraphy of shell concentrations. In: Allison, P.A., Briggs,
871 D.E.G. (eds.), *Taphonomy: Releasing the Data Locked in the Fossil Record*.
872 Plenum Press, New York, 211–290.

873 Kirby, M.X., Jones, D.S., Ávila, S.P., 2007. Neogene shallow-marine
874 paleoenvironments and preliminary Strontium isotope chronostratigraphy of
875 Santa Maria Island, Azores. In: Ávila, S.P. and de Frias Martins, A.M. (eds.),
876 *Proceedings of the 1st Atlantic Islands Neogene. Açoreana Suplemento 5*: 112–
877 125.

878 Kroh, A., Bitner, M.A., Ávila, S.P., 2008. *Novocrania turbinata* (Brachiopoda) from the
879 Early Pliocene of the Azores (Portugal). *Acta Geologica Polonica* 58(4), 473–
880 478.

881 Landau, B., da Silva, C.M., Mayoral, E., 2011. The Lower Pliocene gastropods of the
882 Huelva Sands Formation, Guadalquivir Basin, Southwestern Spain.
883 *Palaeofocus* 4, 1–90.

884 Laughton, A. S., Whitmarsh, R.B., 1974. The Azores-Gibraltar plate boundary. In:
885 Kristjansson, L. (ed.), *Geodynamics of Iceland and the North Atlantic area*,
886 *NATO Advanced Study Institutes Series 11*, 63–81. D. Reidel Publishing
887 Company, Dordrecht.

888 Mayoral, E., Ledesma-Vazquez, J., Baarli, B.G., Santos, A., Ramalho, R, Cachão, M.,
889 Silva, C.M. da, Johnson, M.E., 2013. Ichnology in oceanic islands; case studies
890 from the Cape Verde Archipelago. *Palaeogeography, Palaeoclimatology,*
891 *Palaeoecology* 381–382, 47–66.

892 Madeira, J., Ribeiro, A., 1990. Geodynamic models for the Azores triple junction: a
893 contribution from tectonics. *Tectonophysics* 184 (3–4), 405–415, doi:
894 10.1016/0040-1951(90)90452-E.

895 Madeira, P., Kroh, A., Martins, A.M.F., Ávila, S.P., 2007. The marine fossils from
896 Santa Maria Island (Azores, Portugal): an historical overview. In: Ávila, S.P.,
897 Martins, A.M.F. (eds.), Proceedings of the “1st Atlantic Islands Neogene”,
898 International Congress, Ponta Delgada, 12--14 June 2006. Açoreana
899 Suplemento 5, 59–73.

900 Madeira, P., Kroh, A., Cordeiro, R., Meireles, R., Ávila, S.P., 2011. The fossil
901 echinoids of Santa Maria Island, Azores (Northern Atlantic Ocean). *Acta*
902 *Geologica Polonica* 61(3), 243–264.

903 Marques, F.O., Catalão, J.C., de Mets, C., Costa, A.C.G., Hildenbrand, A., 2013. GPS
904 and tectonic evidence for a diffuse plate boundary at the Azores Triple
905 Junction. *Earth and Planetary Science Letters* 381, 177–187.

906 Mayer, K., 1864. Die Tertiär-Fauna der Azoren und Madeiren. Systematisches
907 Verzeichniss der fossilen Reste von Madeira, Porto Santo und Santa Maria,
908 nebst Beschreibung der neuen Arten. [Edited by author], Zurich, VI+107 pp.

909 McKinney, F.K., Jackson, J.B.C., 1989. *Bryozoan Evolution*. Unwin Hyman, Boston,
910 238 pp.

911 Meireles, R.P., Faranda, C., Gliozzi, E., Pimentel, A., Zanon, V., Ávila, S.P., 2012. Late
912 Miocene marine ostracods from Santa Maria island, Azores (NE Atlantic):
913 Systematics, palaeoecology and palaeobiogeography. *Revue de*
914 *Micropaléontologie* 55(4), 133–148, doi: 10.1016/j.revmic.2012.06.003.

915 Meireles, R.P., Quartau, R., Ramalho, R., Rebelo, A.C., Madeira, J., Zanon, V., Ávila,
916 S.P., 2013. Depositional processes on oceanic island shelves – evidence from
917 storm-generated Neogene deposits from the mid-North Atlantic.
918 *Sedimentology* 60(7), 1769–1785. doi: 10.1111/sed.12055.

- 919 Monegatti, P., Raffi, S., 2001. Taxonomic diversity and stratigraphic distribution of
920 Mediterranean Pliocene bivalves. *Palaeogeography, Palaeoclimatology,*
921 *Palaeoecology* 165(3–4), 171–193. doi: 10.1016/S0031-0182(00)00159-0.
- 922 Monegatti, P., Raffi, S., 2007. Mediterranean-middle eastern Atlantic façade: molluscan
923 biogeography and ecobiostratigraphy throughout the Late Neogene. In: Ávila,
924 S.P., Martins, A.M.F. (eds.), *Proceedings of the 1st Atlantic Islands Neogene.*
925 *Açoreana Suplemento 5*, 126–139.
- 926 Moore, J., Clague, D., Holcomb, R., Lipman, P., Normark, W., Torresan, M., 1989.
927 Prodigious submarine landslides on the Hawaiian Ridge. *Journal of*
928 *Geophysical Research* 94(B12), 17465–17484, doi:
929 10.1029/JB094iB12p17465.
- 930 Nara, M., Seike, K., 2004. *Macaronichnus segregatis*-like traces found in modern
931 foreshore sediments of the Kujukuri-hama Coast, Japan. *Journal of the*
932 *Geological Society of Japan* 110, 545–551.
- 933 Needham, H. D. & Francheteau, J., 1974. Some characteristics of the rift valley in the
934 Atlantic Ocean near 36°48' north. *Earth and Planetary Science Letters*, 22: 29-
935 43.
- 936 Neuendorf, K.K.E., Mehl, Jr., J.P., Jackson, J.A., 2005. *Glossary of Geology.* American
937 Geological Institute, Virginia, 779 pp.
- 938 Oliveira, A.M., Wood, W.L., 1997. Hydrodynamics of bivalve shell entrainment and
939 transport. *Journal of Sedimentary Research* 67(3), 514–526. doi:
940 10.1306/D42685B8-2B26-11D7-8648000102C1865D.
- 941 Pemberton, G.S., Spila, M., Pulham, A.J., Saunders, T., MacEachern, J.A., Robbins, D.,
942 Sinclair, I.K., 2001. *Ichnology and Sedimentology of shallow to marginal*

943 marine systems: Ben Nevis and Avalon Reservoirs, Jeanne D'Arc Basin.
944 Geological Association of Canada, Short Course Notes 15, 343 pp.

945 Piller, W.E., Rasser, M., 1996. Rhodolith formation induced by reef erosion in the Red
946 Sea, Egypt. *Coral Reefs* 15(3), 191–198. doi: 10.1007/BF01145891.

947 Quartau, R., Trenhaile, A.S., Mitchell, N.C., Tempera, F., 2010. Development of
948 volcanic insular shelves: Insights from observations and modelling of Faial
949 Island in the Azores Archipelago. *Marine Geology* 275(1–4), 66–83. doi:
950 10.1016/j.margeo.2010.04.008.

951 Quartau, R., Tempera, F., Mitchell, N.C., Pinheiro, L.M., Duarte, H., Brito, P.O., Bates,
952 R., Monteiro, J.H., 2012. Morphology of the Faial Island shelf (Azores): The
953 interplay between volcanic, erosional, depositional, tectonic and mass-wasting
954 processes. *Geochemistry, Geophysics, Geosystems* 13(4), Q04012. doi:
955 10.1029/2011GC003987.

956 Quartau, R., Mitchell, N.C., 2013. Comment on "Reconstructing the architectural
957 evolution of volcanic islands from combined K/Ar, morphologic, tectonic, and
958 magnetic data: The Faial Island example (Azores)" by Hildenbrand et al.
959 (2012) [*J. Volcanol. Geotherm. Res.* 241–242 (2012) 39–48]. *Journal of*
960 *Volcanology and Geothermal Research* 255, 124–126.

961 Quartau, R., Hipólito, A., Romagnoli, C., Casalbore, D., Madeira, J., Tempera, F.,
962 Roque, C., Chiocci, F.L., 2014. The Morphology of Insular Shelves as a Key
963 for Understanding the Geological Evolution of Volcanic Islands: Insights from
964 Terceira Island (Azores). *Geochemistry, Geophysics, Geosystems* 15, 1801–
965 1826.

966 Quartau, R., Madeira, J., Mitchell, N.C., Tempera, F., Silva P.F. and F. Brandão, 2015
967 (in press). The insular shelves of the Faial-Pico Ridge (Azores archipelago): a

968 morphological record of its geologic evolution. *Geochemistry, Geophysics,*
969 *Geosystems.*

970 Raffi, S., Monegatti, P., 1993. Bivalve taxonomic diversity throughout the Italian
971 Pliocene as a tool for climatic-oceanographic and stratigraphic inferences.
972 *Proceedings of the 1st R.C.A.N.S. Congress, Lisboa, 1992. Ciências da Terra*
973 *12, 45–50.*

974 Ramalho, R., Helffrich, G., Schmidt, D.N., Vance, D., 2010. Tracers of uplift and
975 subsidence in the Cape Verde archipelago. *Journal of the Geological Society*
976 *167(3), 519–538, doi:10.1144/0016-76492009-056.*

977 Ramalho, R., 2011. *Building the Cape Verde Islands.* Springer, Berlin, 262 pp.

978 Ramalho, R., Quartau, R., Trenhaile, A.S., Mitchell, N.C., Woodroffe, C.D., Ávila, S.P.,
979 2013. Coastal evolution in oceanic islands: a complex interplay between
980 volcanism, erosion, sedimentation and biogenic production. *Earth Science*
981 *Reviews, 127: 140–170.*

982 Ramalho, R., Helffrich, G., Madeira, J., Cosca, M., Quartau, R., Thomas, C., Hipólito,
983 A., Ávila, S.P., 2014. The emergence and evolution of Santa Maria Island
984 (Azores) – the conundrum of uplifting islands revisited. *AGU Fall Meeting,*
985 *San Francisco, 15–19 December: Abstract V11B–4697.*

986 Ramalho, R.S., Brum da Silveira, A., Fonseca, P., Madeira, J., Cosca, M., Cachão, M.,
987 Fonseca, M., Prada, S., 2015. The emergence of volcanic oceanic islands on a
988 slow-moving plate: the example of Madeira Island, NE Atlantic. *Geochemistry,*
989 *Geophysics, Geosystems 16, 522–537.*

990 Reineck, H.-E., Singh, I.B., 1973. *Depositional Sedimentary Environments with*
991 *Reference to Terrigenous Clastics.* Springer, Berlin.

992 Santos, A.G., Mayoral, E., da Silva, C.M., Cachão, M., Johnson, M., Baarli, G., 2011.
993 Miocene intertidal zonation on a volcanically active shoreline: Porto Santo in
994 the Madeira Archipelago (Portugal). *Lethaia* 44(1), 26–32, doi:
995 10.1111/j.1502-3931.2010.00222.x.

996 Scarponi, D., Kaufman, D., Amorosi, A., Kowalewski, M., 2013. Sequence stratigraphy
997 and the resolution of the fossil record. *Geology* 41(2), 239–242. doi:
998 10.1130/G33849.1.

999 Schilling, J-G., 1975. Azores mantle blob: rare-earth evidence. *Earth and Planetary*
1000 *Science Letters* 25, 103–115.

1001 Schmincke, H.-U., 2004. *Volcanism*. Springer, Berlin, 324 pp.

1002 Seike, K., 2007. Palaeoenvironmental and palaeogeographical implications of modern
1003 *Macaronichnus segregatis*-like traces in foreshore sediments on the Pacific
1004 coast of central Japan. *Palaeogeography, Palaeoclimatology, Palaeoecology*
1005 252, 497–502.

1006 Serralheiro, A., 1976. A geologia da ilha de Santiago (Cabo Verde). PhD thesis,
1007 Faculdade de Ciências da Universidade de Lisboa.

1008 Serralheiro, A., Alves, C.M., Forjaz, V.H., Rodrigues, B., 1987. Carta Vulcanológica
1009 dos Açores, Ilha de Santa Maria. Centro de Vulcanologia INIC, Ponta Delgada.

1010 Serralheiro, A., Madeira, J., 1990. Stratigraphy and geochronology of Santa Maria
1011 island (Azores). In: *Livro de Homenagem ao Prof. Carlos Romariz*.
1012 Departamento de Geologia da Faculdade de Ciências da Universidade de
1013 Lisboa, Lisboa, 357–376.

1014 Serralheiro, A., 2003. A geologia da ilha de Santa Maria, Açores. *Açoreana* 10, 141–
1015 192.

- 1016 Sibrant, A., Hildenbrand, A., Marques, F.O., Costa, A., 2015. Volcano-tectonic
1017 evolution of the Santa Maria Island (Azores): Implications for paleostress
1018 evolution at the western Eurasia-Nubia plate boundary. *Journal of Volcanology*
1019 and *Geothermal Research* 291, 49–62.
- 1020 Titschack, J., Bromley, R.G., Freiwald, A., 2005. Plio-Pleistocene cliff-bound, wedge-
1021 shaped, warm-temperate carbonate deposits from Rhodes (Greece):
1022 sedimentology and facies. *Sedimentary Geology* 180(1–2), 29–56, doi:
1023 10.1016/j.sedgeo.2005.06.009.
- 1024 Tsutsui, B., Campbell, J.F., Coulbourn, W.T., 1987. Storm-generated, episodic sediment
1025 movements off Kahe Point, Oahu, Hawaii. *Marine Geology* 76, 281–299, doi:
1026 10.1016/0025-3227(87)90034-X.
- 1027 Uchman, A., 1995. Taxonomy and palaeoecology of flysch trace fossils: the
1028 Marnoso–arenacea Formation and associated facies (Miocene, Northern
1029 Apennines, Italy). *Beringeria* 15, 1–115.
- 1030 Uchman, A., 1998. Taxonomy and ethology of flysch trace fossils: revision of the
1031 Marian Ksiazkiewicz collection and studies of complementary material.
1032 *Annales Societatis Geologorum Poloniae* 68(2–3), 105–218.
- 1033 Valentine, J.W., Jablonski, D., Kidwell, S., Roy, K., 2006. Assessing the fidelity of the
1034 fossil record by using marine bivalves. *Proceedings of the National Academy*
1035 *of Sciences* 103(17), 6599–6604, doi: 10.1073/pnas.0601264103.
- 1036 Winkelmann, K., Buckeridge, J.S., Costa, A.C., Dionísio, M.A.M., Medeiros, A.,
1037 Cachão, M., Ávila, S.P., 2010. *Zullobalanus santamariaensis* sp. nov., a new
1038 late Miocene barnacle species of the family Archeobalanidae (Cirripedia:
1039 Thoracica), from the Azores. *Zootaxa* 2680, 33–44.

1040 Wisshak, M., Form, A., Jakobsen, J., Freiwald, A., 2010. Temperate carbonate cycling
1041 and water mass properties from intertidal to bathyal depths (Azores).
1042 *Biogeosciences* 7, 2379–2396, doi:10.5194/bg-7-2379-2010.

1043 Wisshak, M., Tribollet, A., Golubic, S., Jakobsen, J., Freiwald, A., 2011. Temperate
1044 bioerosion: ichnodiversity and biodiversity from intertidal to bathyal depths
1045 (Azores). *Geobiology* 9(6), 492–520, doi: 10.1111/j.1472-4669.2011.00299.x.

1046 Wisshak, M., Berning, B., Jakobsen, J., Freiwald, A., 2014. Temperate carbonate
1047 production: biodiversity of calcareous epiliths from intertidal to bathyal depths
1048 (Azores). *Marine Biodiversity*, doi 10.1007/s12526-014-0231-6.

1049 Zazo, C., Goy, J.L., Hillaire-Marcel, C., Gillot, P.-Y., Soler, V., González, J.Á., Dabrio,
1050 C.J., Ghaleb, B., 2002. Raised marine sequences of Lanzarote and
1051 Fuerteventura revisited – a reappraisal of relative sea-level changes and vertical
1052 movements in the eastern Canary Islands during the Quaternary. *Quaternary*
1053 *Science Reviews* 21(18–19), 2019–2046. doi: 10.1016/S0277-3791(02)00009-
1054 4.

1055 Zazo, C., Goy, J.L., Dabrio, C.J., Soler, V., Hillaire-Marcel, C., Ghaleb, B., González-
1056 Delgado, J.A., Bardají, T., Cabero, A., 2007. Quaternary marine terraces on Sal
1057 Island (Cape Verde archipelago). *Quaternary Science Reviews* 26(7–8), 876–
1058 893, doi: 10.1016/j.quascirev.2006.12.014.

1059 Zazo, C., Goy, J.L., Hillaire-Marcel, C., Dabrio, C.J., González-Delgado, J.A., Cabero,
1060 A., Bardají, T., Ghaleb, B., Soler, V., 2010. Sea level changes during the last
1061 and present interglacials in Sal Island (Cape Verde archipelago). *Global and*
1062 *Planetary Change* 72(4), 302–317, doi: 10.1016/j.gloplacha.2010.01.006.

1063 Zbyszewski, G., da Veiga Ferreira, O., 1962. La faune Miocène de l'île de Santa Maria
1064 (Açores). *Comunicações dos Serviços Geológicos de Portugal* 46, 247–289.

1065

1066 **Figures and tables**

1067

1068 **Fig. 1.** Location maps. **Insert.** Location of the Azores Archipelago within the NE
1069 Atlantic. MAR = Mid-Atlantic Ridge; NA = North American plate; Nu – Nubian
1070 (African) plate; Eu = Eurasian plate. Location of Santa Maria, within the Azores
1071 Archipelago.

1072

1073 **Fig. 2. A.** Simplified geological map of Santa Maria (Serralheiro et al., 1987;
1074 Serralheiro, 2003). **B.** Profile of Santa Maria Island (vertical amplification = 3x). **C.**
1075 Pedra-que-pica on SE Santa Maria (white rectangle).

1076

1077 **Fig. 3. A–B.** Position of the rocky spurs in relation to the Pedra-que-pica fossiliferous
1078 sediments. **A.** White asterisks mark the position of the calcareous sand inclusions, some
1079 of which feature examples of the trace fossil *Macaronichnus segregatis*, on the rocky
1080 spurs. The four red flags indicate the location of the diving where rock samples were
1081 collected. Hatch white line represents the present exposed area of the coquina.
1082 Continuous hard white line represents the total inferred area of the coquina. **B.** Pedra-
1083 que-pica seen from the east (lateral view).

1084

1085 **Fig. 4.** Stratigraphy and sedimentological structures at Pedra-que-pica. **A.** General
1086 cross-section of Pedra-que-pica volcano-sedimentary sequence, showing the
1087 volcanostratigraphic setting of the basal sedimentary sequence, and location of the
1088 passage zone between subaerial and submarine flows (representing coeval sea-level)
1089 within the overlying lava delta sequence. **B.** Stratigraphic framework and interpretation
1090 of the Pedra-que-pica lithological succession. The numbers depicted in black circles

1091 correspond to facies 1–8, which are described in the text. The scale bar indicates the
1092 location of the detailed composite profile (see Figure 5).

1093

1094 **Fig. 5.** Detailed composite stratigraphic column at Pedra-que-pica (N36°55.806'',
1095 W25°01.482''). The numbers depicted in black circles correspond to facies 1–6, which
1096 are described in the text.

1097

1098 **Fig. 6.** Remnant sediments and their trace fossils on the pre-existing topography, below
1099 the coquina. **A–B.** Light grey calcarenites forming sandstone pockets up to 1 m thick,
1100 bioturbated with abundant *Macaronichnus segregatis* and rare ?*Ophiomorpha* isp., rest
1101 directly on the bedrock. Note that part of the sediments (the shell rich parts), belong to
1102 the overlaying coquina. **C–D.** Neptunian dikes filled with calcareous sand and
1103 bioturbated by *Macaronichnus segregatis*.

1104

1105 **Fig. 7.** Selected sedimentary features of the coquina and associated deposits. **A.** General
1106 view of the coquina at Pedra-que-pica seen from the west. **B.** Coquina resting directly
1107 on top of the basal pillow lavas of the Touril Complex (eastern section of the outcrop).
1108 **C.** General view of the first coquina layer (facies 3a) seen from the east. Note the
1109 chaotic disposition of the smaller ostreid shells and the valve of a large *Gigantopecten*
1110 *latissimus* in a vertical position (center of the photo). **D.** Closer view of the
1111 conglomerate layer that separates coquina deposits formed by two debris-fall events.
1112 The conglomerate is a moderately-sorted, component-supported volcanoclastic pebble to
1113 cobble sediment (facies 3b) located ~1 m from the base of the sedimentary Touril
1114 succession at Pedra-que-Pica. The intermediate conglomerate contains a volcanoclastic

1115 calcarenite matrix, similar to the matrix of the overlying coquina. **E.** General view of
1116 the second coquina layer (facies 3c) seen from the west.

1117

1118 **Fig. 8.** Selected sedimentary features of the coquina and associated deposits. **A.** Broken
1119 test of an echinoderm *Clypeaster altus*. **B.** Rhodolith. **C.** Bryolith bioeroded by the
1120 bivalve *Myoforceps aristatus*. **D.** The coquina seen from the above. **E.** One of the very
1121 rare *Gigantopecten latissimus* with the two valves still articulated. **F.** Calcarenite
1122 (topmost section of the coquina). **G.** *Bichordites* isp., a trace fossil produced by
1123 burrowing spatangoid echinoids. **H.** Sandstones bioturbated by *Asterosoma* isp. (eastern
1124 section of Pedra-que-pica).

1125

1126 **Fig. 9. A–B.** Cross sections of bulk samples of the coquina. **A.** submarine sample. **B.**
1127 Subaerial sample. **C–H.** Thin sections illustrating the lithologies found in facies 3 and 4.
1128 **C–D.** Volcaniclastic calcarenite matrix of the coquina-rudstone. **E.** Matrix (tuffaceous
1129 sandstone) of the water settled tuff. **F–H.** Sections of lithoclasts floating in the water-
1130 settled tuff matrix. **F.** Mudstone/siltstone lithoclast with numerous bioclasts and lithic
1131 fragments. **G.** Volcaniclastic sandstone with abundant bioclasts. **H.** Limestone lithoclast
1132 (coarse biosparite with subordinate lithic fragments). Aragonite gastropods are visible in
1133 the center of the photo. Scale bars equal to 1 mm.

1134

1135 **Fig. 10. A.** Coquina (light yellow, bottom unit) overlaid by well-stratified, fine- to
1136 coarse-grained vitric ash to lapilli water-settled tuffs. **B.** Fluid-escape structure (facies
1137 4) at the base of the tuffs. **C.** External mould of a bivalve (facies 4). **D.** Non-ballistically
1138 emplaced pebble (facies 4).

1139

1140 **Fig. 11.** Stratigraphic logs covering the shell accumulations in the coquina. A bimodal
1141 distribution is clearly visible, with most of the big bivalve *Gigantopecten* valves
1142 concordant (oriented concave-down) and with the small valves of *Ostrea* spp. and of
1143 other bivalve species mainly concordant but with high numbers of valves also in
1144 unstable positions (perpendicular and oblique). **A-C.** Rose diagrams for the 1,482
1145 valves of ostreids (counted on the three vertical logs). **D.** Rose diagram for the 389
1146 valves of *Gigantopecten latissimus* (counted along the entire outcrop; top right). The
1147 angles of the shells for the construction of the rose diagrams were measured according
1148 to the figure. The tallest person (in grey) is about 1.80 m.

1149

1150 **Fig. 12.** Depositional model inferred for the formation of a coquina in the context of an
1151 insular shelf using Pedra-que-pica as an example (figure not to scale). **A.** Formation of
1152 the basal carbonate sand with abundant *Macaronichnus segregatis* Clifton and
1153 Thompson, 1978, during lower but rapidly rising relative sea-level. **B.** Sea-level rise and
1154 establishment of a shallow-water carbonate factory during stand-still. Debris-fall
1155 transport from shallow-water carbonate factory onto deeper parts of the shelf (~50 m
1156 depth) possibly triggered by storm events. **C.** Waning of storm event and gradual
1157 establishment of fair-weather conditions allowing the deposition of finer sediments (fine
1158 sand), thickening against the rocky spur that acts like a coastal groin. **D.** Fair-weather
1159 conditions. Bioturbation of the top calcarenites by opportunistic invertebrate organisms.

1160

1161

1162 **Table 1.** Taxa found at Pedra-que-pica outcrop.

1163

1164 Table 1: Taxa of fossils found at Pedra-que-pica outcrop.

GROUP	Taxa
Brachiopoda	<i>Novocrania turbinata</i> (Poli, 1795)
Bryozoa	<i>Antropora</i> sp. <i>Biflustra</i> sp. <i>Bryopesanser</i> sp. <i>Buffonellaria</i> sp. <i>Caberea</i> sp. <i>Calloporina</i> sp. Celleporidae indet. Chaperiidae indet. <i>Chaperiopsis</i> sp. <i>Cheiloporina</i> sp. <i>Chorizopora</i> sp. ? <i>Crassimarginatella</i> sp. <i>Crepidacantha</i> sp. <i>Cryptosula</i> sp. <i>Escharella</i> sp. <i>Escharina</i> sp. <i>Escharoides</i> sp. <i>Figularia</i> cf. <i>figularis</i> (Johnston, 1847) <i>Hincksina</i> sp. ? <i>Hippaliosina</i> sp. <i>Hippopleurifera</i> sp. <i>Metroperiella</i> sp. <i>Microporella</i> sp. 1 <i>Microporella</i> sp. 2 " <i>Myrizoum</i> " cf. <i>marionense</i> Busk, 1884 <i>Onychocella</i> cf. <i>angulosa</i> (Reuss, 1847) ? <i>Plesiocleidochasma</i> sp. <i>Puellina</i> (<i>Glabrilaria</i>) sp. <i>Puellina</i> (<i>Puellina</i>) sp. 1 <i>Puellina</i> (<i>Puellina</i>) sp. 2 <i>Reteporella</i> sp. <i>Saevitella</i> sp. <i>Schizomavella</i> cf. <i>triaviculata</i> (Calvet, 1903) <i>Schizotheca</i> sp. <i>Scrupocellaria</i> sp. <i>Smittoidea</i> sp. <i>Therenia</i> sp. ? <i>Umbonula</i> sp.
Cnidaria, Anthozoa	<i>Porites</i> sp.
Crustacea	? <i>Megabalanus</i> sp. <i>Zullobalanus santamariaensis</i> Buckeridge & Winkelmann, 2010
Echinodermata	<i>Clypeaster altus</i> (Leske, 1778)

	<i>Echinocyamus pusillus</i> (Müller, 1776)
	<i>Echinoneus</i> cf. <i>cyclostomus</i> Leske, 1778
	<i>Eucidaris tribuloides</i> (Lamarck, 1816)
	<i>Schizobrissus</i> sp.
	Spatangoida indet.
Mollusca, Gastropoda	<i>Cheilea equestris</i> (Linnaeus, 1758)
	<i>Cirsotrema</i> cf. <i>cochlea</i> (G. B. Sowerby II, 1844)
	<i>Persististrombus</i> sp.
Mollusca, Bivalvia	<i>Aequipecten opercularis</i> (Linnaeus, 1758)
	<i>Anadara</i> sp.
	<i>Arca noae</i> Linnaeus, 1758
	<i>Argopecten</i> cf. <i>levicostatus</i> Toulou, 1909 = <i>Pecten</i> cf. <i>laevicostatus</i> (G. B. Sowerby II, 1844,)
	<i>Chlamys hartungi</i> (Mayer, 1864)
	<i>Cubitostrea frondosa</i> (de Serres, 1829) = <i>Ostrea frondosa</i> de Serres, 1829
	<i>Gigantopecten latissimus</i> (Brocchi, 1814)
	<i>Lopha plicatuloides</i> (Mayer, 1864)
	<i>Manupecten pesfelis</i> (Linnaeus, 1758)
	<i>Myoforceps aristatus</i> (Dillwyn, 1817)
	<i>Ostrea</i> cf. <i>lamellosa</i> Brocchi, 1814
	<i>Pecten dunkeri</i> Mayer, 1864
	<i>Spondylus</i> cf. <i>concentricus</i> Bronn, 1831
	<i>Spondylus gaederopus</i> Linnaeus, 1758
	<i>Talochlamys abscondita</i> (Fischer in Locard, 1898) = <i>Hinnites ercolanianus</i> (Cocconi, 1873)
Chordata, Actinopterygii	<i>Sparus cinctus</i> Agassiz, 1839
Chordata, Elasmobranchii	<i>Carcharhinus</i> cf. <i>leucas</i> (Valenciennes, 1839 in Müller and Henle, 1839–1841)
	<i>Cosmopolitodus hastalis</i> (Agassiz, 1833)
Chordata, Mammalia	Cetacea indet.

1165

1166

1167

Figure 1
[Click here to download high resolution image](#)

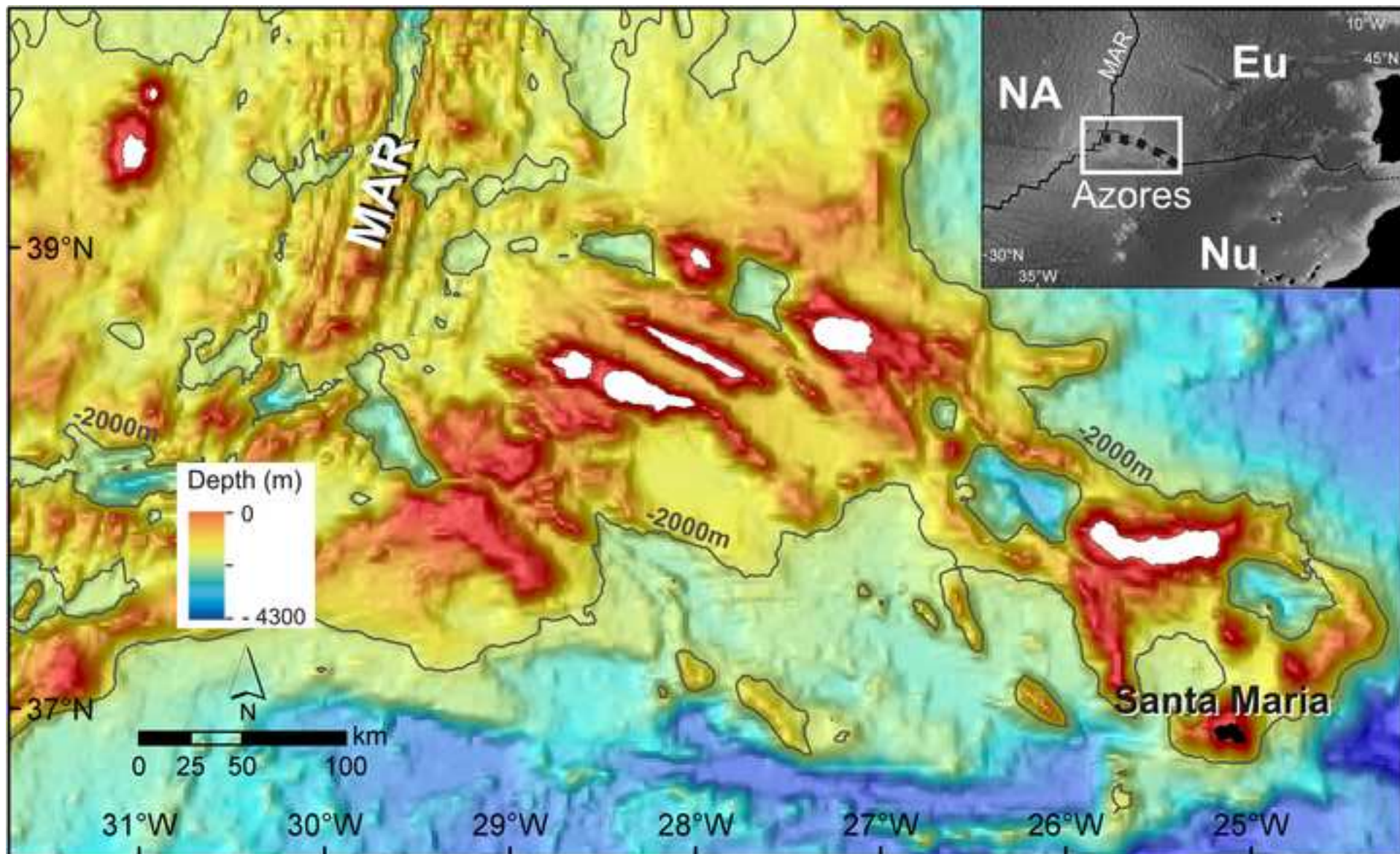


Figure 2

[Click here to download high resolution image](#)

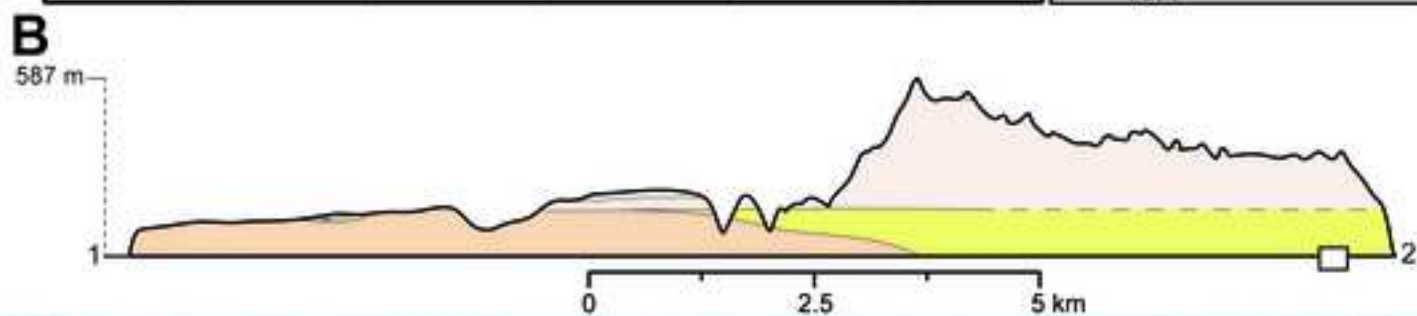
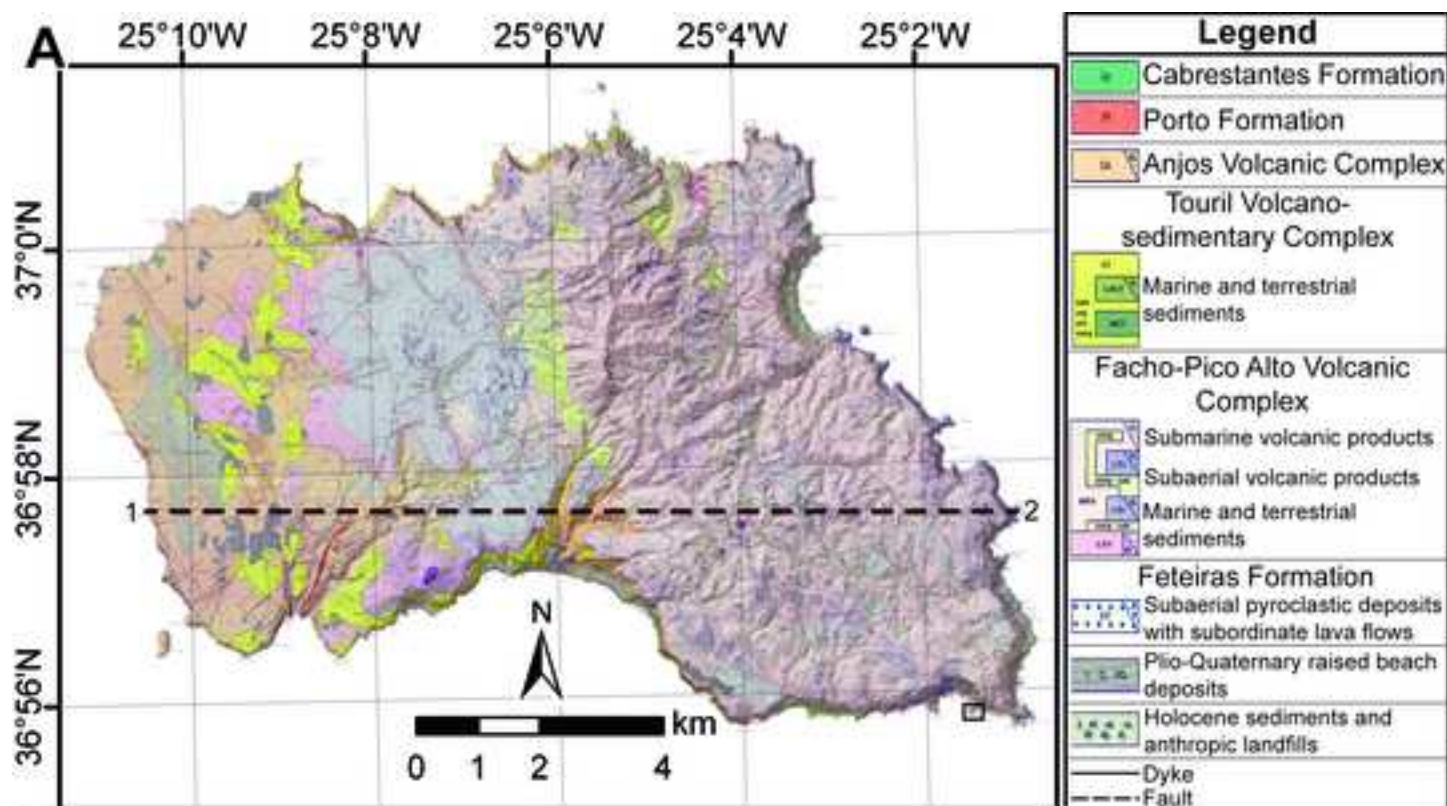


Figure 3
[Click here to download high resolution image](#)



Figure 4
[Click here to download high resolution image](#)

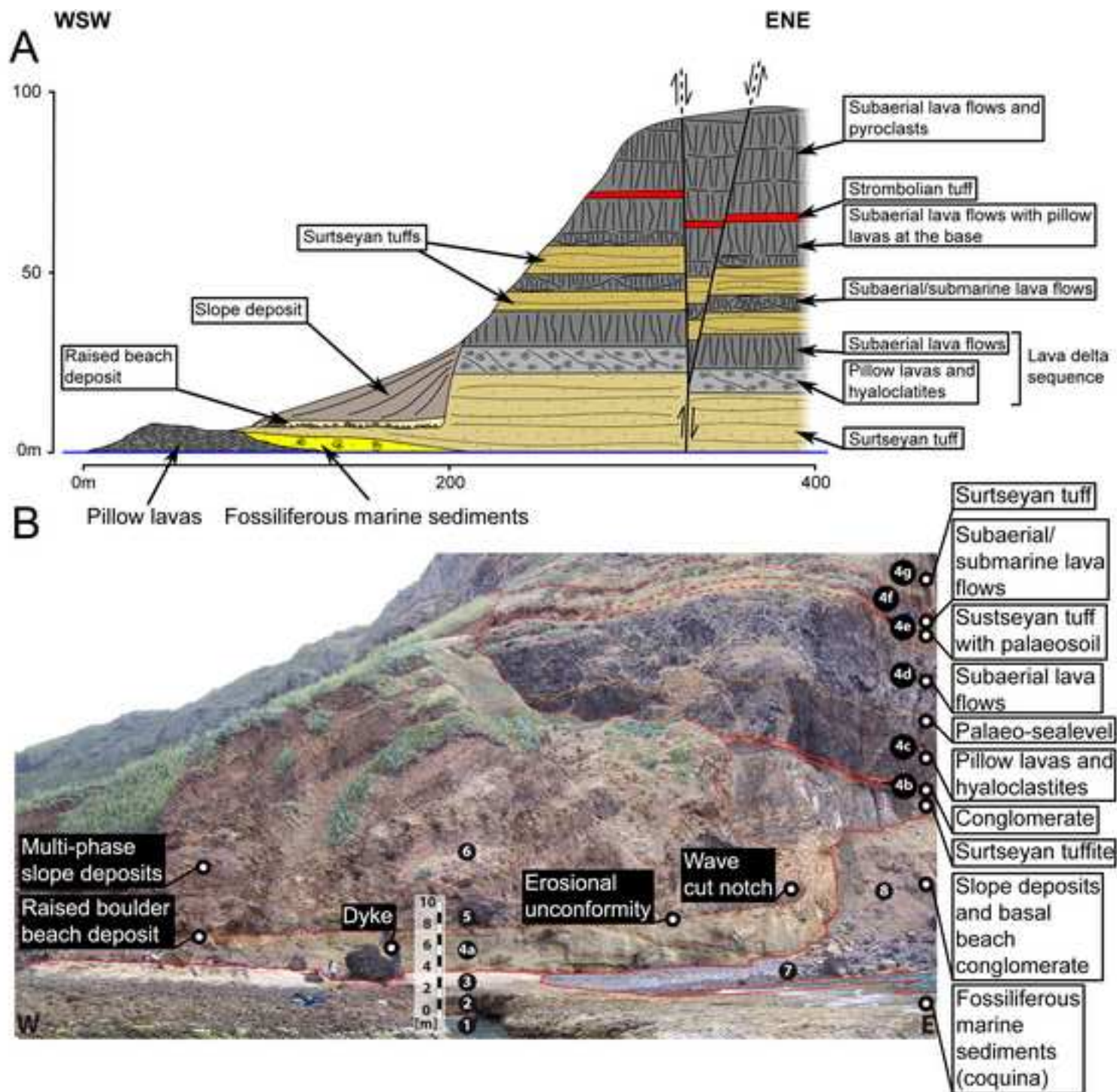


Figure 5
[Click here to download high resolution image](#)

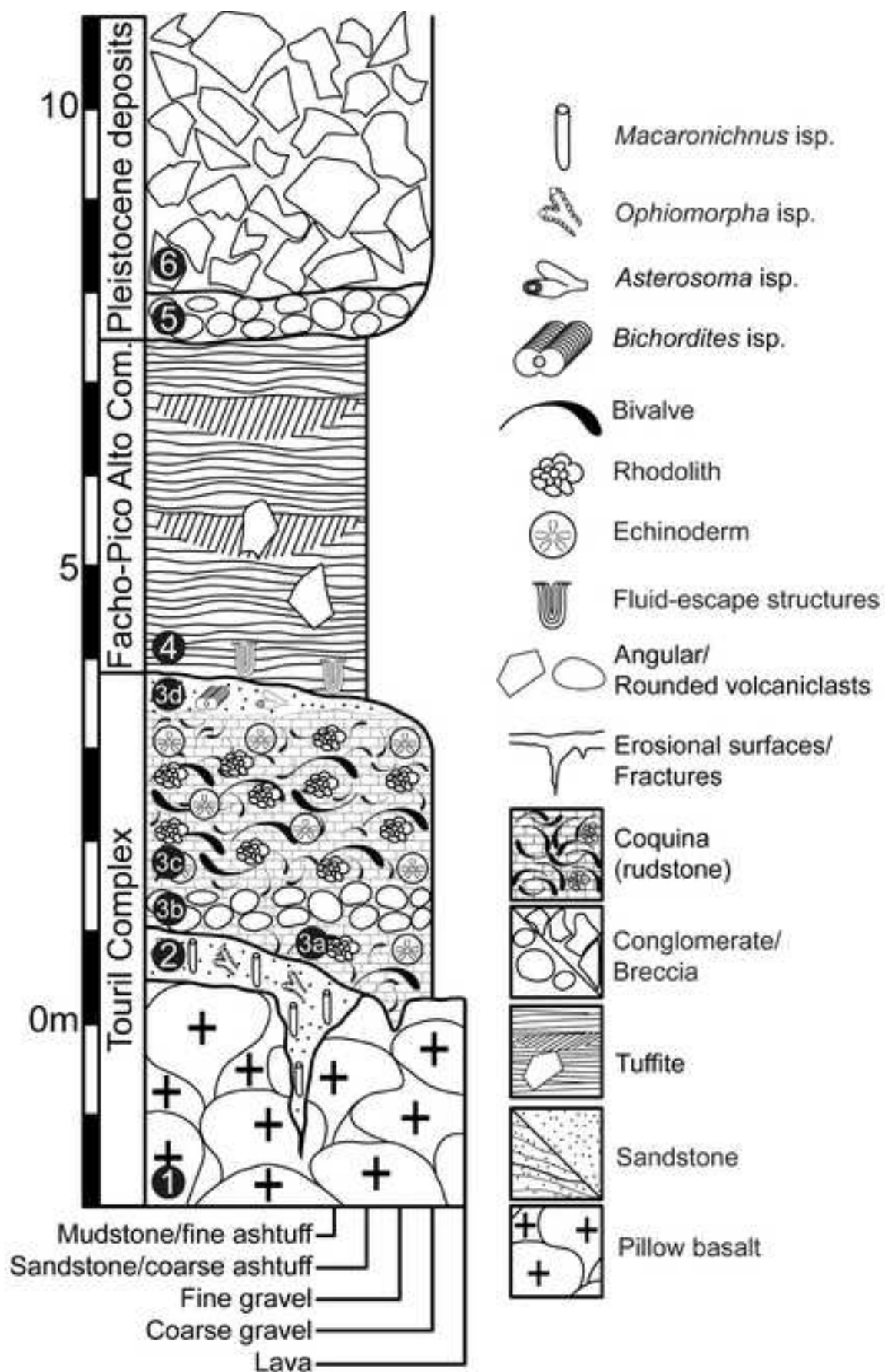


Figure 6
[Click here to download high resolution image](#)



Figure 7
[Click here to download high resolution image](#)



Figure 8
[Click here to download high resolution image](#)

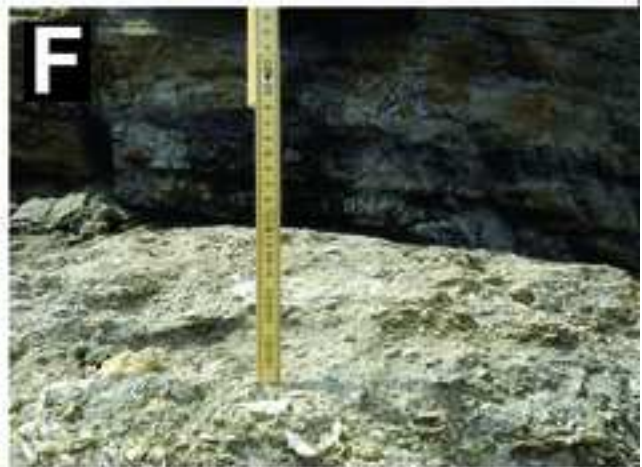


Figure 9
[Click here to download high resolution image](#)

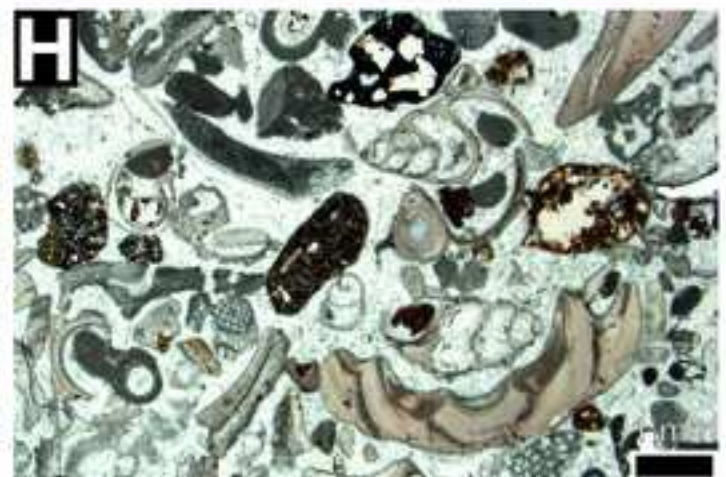
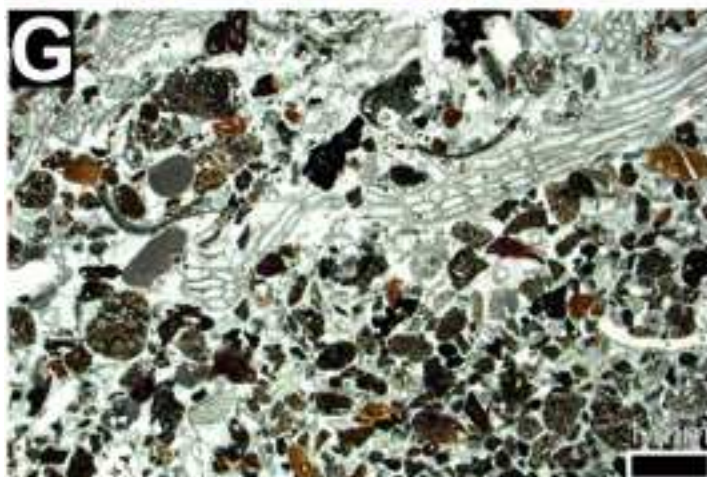
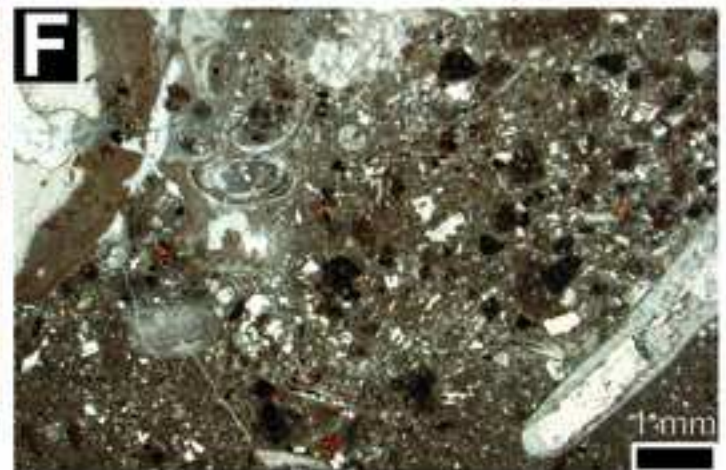
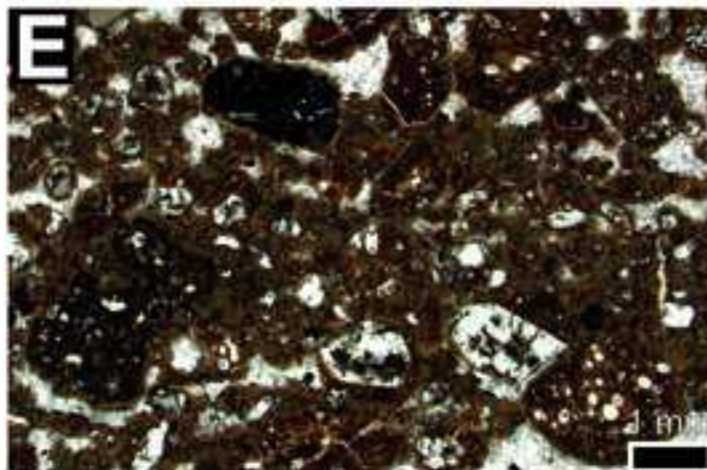
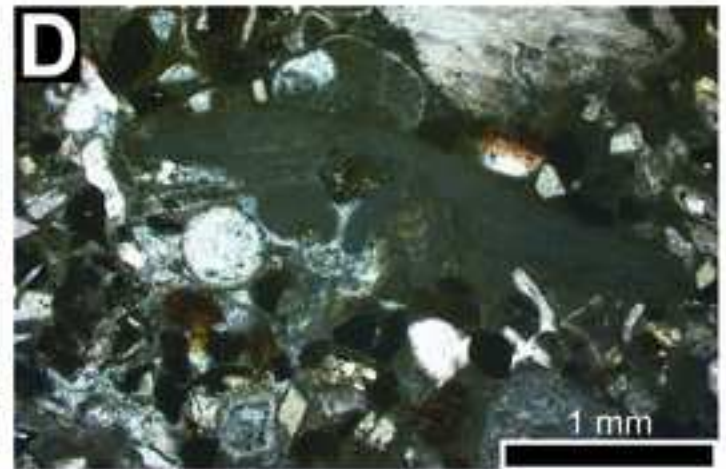
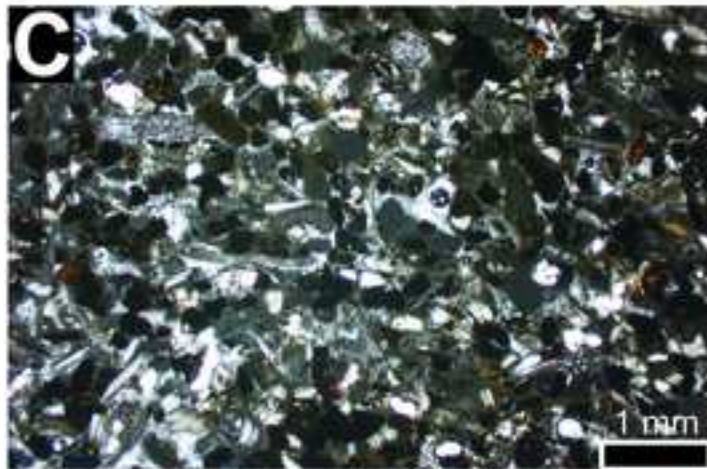
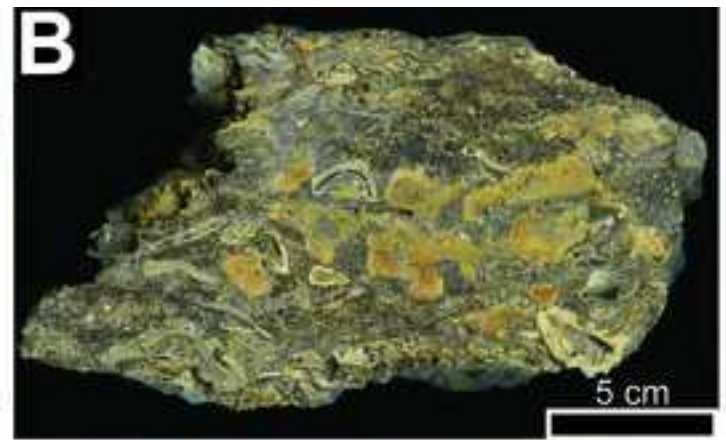


Figure 10
[Click here to download high resolution image](#)



Figure 11
[Click here to download high resolution image](#)

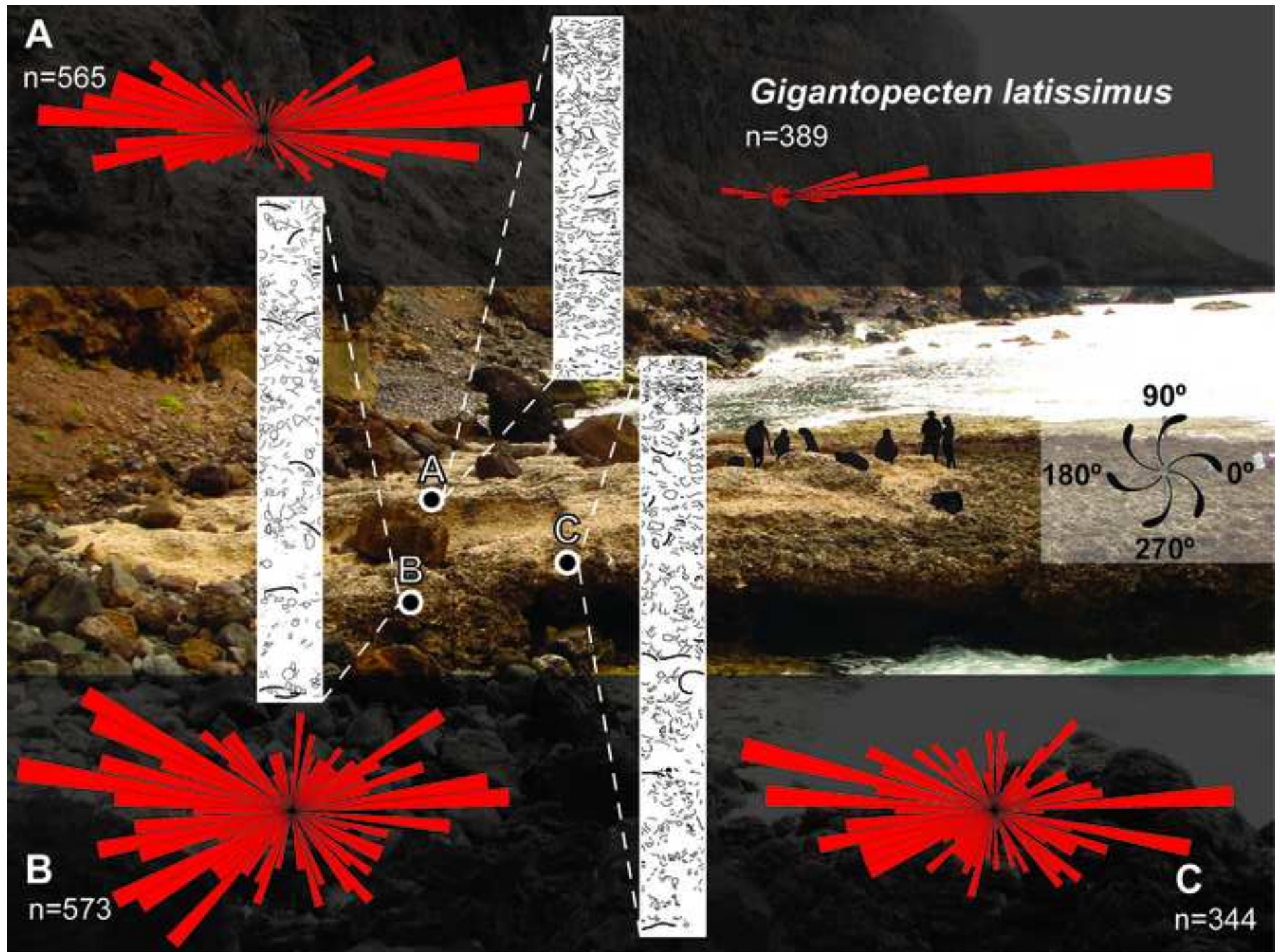


Figure 12
[Click here to download high resolution image](#)

